



MINISTRY OF AVIATION

AERONAUTICAL RESEARCH COUNCIL

CURRENT PAPERS

An Empirical Prediction Method
for Non-Linear Normal Force on
Thin Wings at Supersonic Speeds

by

J. R. Collingbourne

LONDON: HER MAJESTY'S STATIONERY OFFICE

1963

PRICE 7s 6d NET

U.D.C. No. 533.693 : 533.6.011.5 : 533.6.013.13

C.P. No. 662

January, 1962

AN EMPIRICAL PREDICTION METHOD FOR NON-LINEAR NORMAL FORCE
ON THIN WINGS AT SUPERSONIC SPEEDS

by

J.R. Collingbourne

SUMMARY

Theoretical and experimental results are used to produce a coherent 'engineering' method for predicting normal force on thin sharp-edged wings at supersonic speeds, the initial force curve slope being known. The method can be applied at angles up to 90° and, in principle, to any planform, although most of the results used to develop the method are for delta and rectangular wings.

A summary of the method is given in section 5.

LIST OF CONTENTS

	<u>Page</u>
1 INTRODUCTION	1
2 NORMAL FORCE ON UPPER SURFACE	2
2.1 The hypersonic non-linear factor $(b_u)_h$	6
2.2 The leading edge vortex factor $(b_u)_v$	7
2.3 Upper surface force as a function of Ma and Ma_u	8
3 NORMAL FORCE ON LOWER SURFACE	9
3.1 Lower surface force with shock detached, $C_{N\ell}'$	11
3.2 Lower surface force with shock attached, $C_{N\ell}^x$	12
3.3 Lower surface force with shock 'partially attached', $C_{N\ell}' + \Delta C_{N\ell}$	14
4 COMPARISONS BETWEEN ESTIMATED AND MEASURED NORMAL FORCE	15
5 SUMMARY OF METHOD	16
6 CONCLUSIONS	17
LIST OF SYMBOLS	17
LIST OF REFERENCES	19

ILLUSTRATIONS (Figs. 1 - 13c)

DETACHABLE ABSTRACT CARDS

LIST OF ILLUSTRATIONS

	<u>Fig.</u>
Normal force on upper surface of flat plate in two dimensional flow	1
The leading edge vortex normal force factor $(b_u)_v$ as a function of Mach No. normal to mean swept edge, for thin, sharp edged wings at supersonic speeds	2
Mach No. normal to mean swept edge at zero incidence, as a function of Ma, for various slender wings	3
The leading edge vortex normal force factor $(b_u)_v$ as a function of Ma and Ma_u for thin, sharp-edged wings at supersonic speeds	4
Normal force on upper surface of thin, sharp-edged wings at supersonic speeds, as a function of Ma and Ma_u	5
Construction of $C_{N\ell}$ vs. α_ℓ curve	6
Lower surface incidence for shock detachment, α_ℓ^* , for thin, sharp-edged wings	7
Normal force coefficient on lower surface of thin wings at 90° incidence	8
Ratio of $C_{N\ell}^x$ in two-dimensional flow, as estimated by equation (19) and by oblique shock equations	9

LIST OF ILLUSTRATIONS (Contd)

	<u>Fig.</u>
Normal force coefficient on the lower surface of thin, sharp-edged wings with leading edge shock attached	10
Lower surface normal force at angles above shock detachment	11
Comparison between estimated and measured C_N vs. α for Delta wings with leading edge shock detached, or α_c^* small	12
Comparison between estimated and measured C_N vs. α for wings with $\alpha_c^* > 5^\circ$ (leading edge shock attached case)	
(a) Rectangular wings, $\beta A > 2$	13(a)
(b) Rectangular wings, $\beta A < 2$ (interfering tips)	13(b)
(c) Delta wings	13(c)

1 INTRODUCTION

For preliminary design work it is essential to have a convenient method available for the rapid estimation of the normal force developed on simple wings. Methods based on linearised theory are well known, but in the case of some aircraft and most guided weapons designed to operate at supersonic speeds, the maximum angles of incidence used are greater than those at which it is reasonable to assume a linear relationship between normal force coefficient and incidence, and it becomes necessary to take account of the non-linearities. In the case of guided weapons, angles of incidence up to 25° are not uncommon, and weapons or space vehicles designed to operate at very high altitudes may adopt angles of incidence considerably in excess of this.

Besides its relevance to estimates of acceleration capability and drag due to incidence, a knowledge of normal force at high angles of incidence is a prerequisite for estimates of various aerodynamic moments which are essentially associated with normal force.

The following method for the approximate estimation of normal force is semi-empirical, and is offered partly as a basis for discussion and further refinement, and also as an interim engineering method which is simple and consistent with existing theoretical and experimental results. It will be assumed that the initial force curve slope is known, the problem being to estimate the non-linear force.

It is proposed to treat the contributions to normal force from the upper and lower surfaces quite separately, i.e.

$$C_N = C_{Nu} + C_{Nl} \quad (1)$$

where suffices ()_u and ()_l refer to upper and lower wing surfaces respectively. Following the predictions of linearised theory it will further be assumed that

$$(C_{Nu})_{\alpha \rightarrow 0} = \frac{a}{2} \cdot \alpha_u$$

$$(C_{Nl})_{\alpha \rightarrow 0} = \frac{a}{2} \cdot \alpha_l$$

where $a = (dC_N/d\alpha)_{\alpha \rightarrow 0}$, α is the incidence of the mean chord plane and α_u , α_l are the incidence angles of the upper and lower surfaces respectively. For thin wings with sharp trailing edges, α_u , α_l and α are equal, but for wings having a finite mean trailing edge thickness/chord \bar{d}/c , then α_u , α_l are defined by

$$\left. \begin{aligned} \alpha_u &= \alpha - \frac{\bar{d}}{2c} \\ \alpha_l &= \alpha + \frac{\bar{d}}{2c} \end{aligned} \right\} \quad (2)$$

For the purpose of this analysis it is proposed to assume that effects of thickness (other than at the trailing edge) can be neglected. It is believed that thickness distribution may have an appreciable effect on the non-linear force components, especially in the case of very slender wings; hence consideration will be restricted in the main to wings with sharp leading edges and thickness/chord ratios less than about 5%.

2 NORMAL FORCE ON UPPER SURFACE

Two distinct reasons can be found why the variation of normal force on the upper surface should not be linear with incidence. The overriding reason is that the upper surface force cannot exceed a value corresponding to the attainment of zero pressure over the surface, so that the relationship between normal force and incidence must exhibit a maximum. Hence there must be a non-linear force component which causes the upper surface normal force ultimately to fall below the linear prediction and have the correct maximum value. Since it can be shown from two-dimensional flow theory that this component depends on the hypersonic parameter Ma , it will be referred to generally as the hypersonic non-linear force component for the upper surface.

The second component of non-linear force which is associated in the main with the upper surface flow is that which arises from the action of the coiled vortex sheets shed from swept leading edges and tips. This component is only present in the case of slender wings for which the mean Mach. No. normal to the leading and tip edges is subsonic; it will be referred to as the non-linear force component due to leading edge vortices. Unlike the hypersonic component, it causes an increase in force above the linear prediction, but only at angles of incidence well below that at which the hypersonic vacuum limit is approached.

At angles of incidence below $\hat{\alpha}_u$ (the incidence at which the upper surface normal force coefficient reaches its maximum value), it is proposed to assume that the relation between upper surface normal force and incidence can be expressed as follows

$$C_{Nu} = \frac{a}{2} \alpha_u + b_u \alpha_u^2 \quad (\alpha_u < \hat{\alpha}_u) \quad (3)$$

This general form for the equation has been chosen because it is consistent with two-dimensional flow theory for angles of incidence not too close to $\hat{\alpha}_u$, as shown in section 2.1 below. For $\alpha_u > \hat{\alpha}_u$, C_{Nu} is constant and equal to its maximum value, \hat{C}_{Nu} , which will be taken to be a fraction k of the negative pressure coefficient corresponding to absolute vacuum,

$$\hat{C}_{Nu} = k(-C_p)_{vac} = \frac{2k}{\gamma M^2} \quad (\alpha_u > \hat{\alpha}_u) \quad (4)$$

As outlined above, the upper surface non-linear force has two distinct origins and it is therefore proposed to assume that b_u is the sum of two components associated with each, i.e.

$$b_u = (b_u)_h + (b_u)_v \quad (5)$$

$(b_u)_h \alpha_u^2$ and $(b_u)_v \alpha_u^2$ are the hypersonic and leading edge vortex components respectively of the upper surface non-linear force coefficient. It is clear that since the factor $(b_u)_h$ is associated with the maximum value of C_{Nu} , $(b_u)_v$ must be a function of incidence having the characteristics that it does not affect \hat{C}_{Nu} and is zero for $\alpha_u > \hat{\alpha}_u$.

Methods for evaluating $(b_u)_h$ and $(b_u)_v$ are described below, in sections 2.1 and 2.2 respectively.

2.1 The hypersonic non-linear factor, $(b_u)_h$

From equations (3) and (4), and the prescribed condition that the non-linear component due to leading edge vortices shall not affect \hat{C}_{Nu} , it follows that

$$\left. \begin{aligned} (b_u)_h &= -\frac{\gamma(Ma)^2}{32k} && \text{for } \alpha < \hat{\alpha}_u \\ (b_u)_h &= -\left(\frac{Ma}{2M\hat{\alpha}_u} - \frac{2k}{\gamma(M\hat{\alpha}_u)^2}\right) && \text{for } \alpha_u > \hat{\alpha}_u \end{aligned} \right\} (6)$$

where
$$M\hat{\alpha}_u = \frac{8k}{\gamma Ma} \quad (7)$$

It has been pointed out by Relf¹, Mayer² and others that $(-C_p)_{\max}/(-C_p)_{\text{vac}}$, the ratio of the maximum negative pressure coefficient achieved on wings or bodies to that corresponding to vacuum is remarkably constant over a wide range of Mach Nos. from subsonic to hypersonic. The most frequently quoted value for the ratio is 0.7, although slightly higher values are sometimes measured. Since any departure from a value of unity is presumably an effect of viscosity the ratio may depend on the state of the boundary layer. Now the mean suction on the upper surface of a wing arises from the effects of both thickness and incidence, and hence the appropriate value of k in equations (4), (6), (7) will be less than $(-C_p)_{\max}/(-C_p)_{\text{vac}}$ by an amount $(-\bar{C}_p)_t/(-C_p)_{\text{vac}}$, where $(-\bar{C}_p)_t$ is the mean negative pressure coefficient due to thickness. Since this analysis is expressly concerned with thin wings, it is proposed to assume $k = 0.7$ for all cases, (except where otherwise stated), which is tantamount to overestimating C_{Nu} by an amount $(-\bar{C}_p)_t$ if $\alpha_u > \hat{\alpha}_u$, the error being less for $\alpha_u < \hat{\alpha}_u$. This error is unlikely to be significant in the case of wings with supersonic leading edges, since in two-dimensional flow $(-\bar{C}_p)_t \approx 0$, but clearly thickness may have an important effect in reducing C_{Nu} on wings with subsonic leading edges.

The validity of equations (3) and (6) can be checked in the particular case of two-dimensional flow (for which $(b_u)_v = 0$ and

$b_u = (b_u)_h$) by comparing the empirical prediction of C_{Nu} for this case with exact Prandtl-Meyer values for inviscid flow. This comparison is made in Fig. 1, by plotting the force coefficients in two-dimensional flow in the form

$$M^2(C_{Nu})_{2D} = f[M(a)_{2D} \cdot M\alpha_u] \quad (8)$$

For $\alpha_u < \hat{\alpha}_u$ the empirical prediction (equations (3) and (6)) cast in this form is

$$M^2(C_{Nu})_{2D} = \frac{1}{2} M(a)_{2D} \cdot M\alpha_u - \frac{\gamma}{32k} [M(a)_{2D} \cdot M\alpha_u]^2 \quad (9)$$

The full lines in Fig. 1 show this prediction for two typical values of k , 0.7 and 0.75, while the exact Prandtl-Meyer values are plotted as points for various Mach Nos. and angles. It will be noted, first that equation (8) correlates the theoretical results extremely well, and second that with these observed values of k , equation (9) predicts the theoretical values with good accuracy at angles up to about $2/3 \hat{\alpha}_u$. At higher angles of course the empirical curve falls below the theoretical values since the latter tend to the absolute vacuum maximum, never attained in practice.

Equations (6) and (7) show that $(b_u)_h$ depends on the parameters Ma and $M\alpha_u$. Since $(a)_{2D} \rightarrow 4/M$ as $M \rightarrow \infty$, equation (8) takes the well-known hypersonic similarity form for $M \gg 1$, and $M\hat{\alpha}_u$ then has the value unity with $k = 0.7$.

2.2 The leading edge vortex factor, $(b_u)_v$

The quantity $(b_u)_v \cdot \alpha_u^2$ is the increment in normal force coefficient due to the action of the vortex sheets which spring from the swept leading and tip edges when the flow separates from these edges. The theoretical studies of Mangler and Smith³ give $(b_u)_v \simeq 4$ for the case of a slender delta wing for which the slenderness parameters $\beta \cot \Omega_0$ and $\beta \alpha$ tend to zero, where $\beta = \sqrt{M^2 - 1}$ and Ω_0 is the leading edge sweepback. In a comprehensive survey of flow round swept edges, Stanbrook and Squire⁴ have observed that at moderate angles of incidence ($M\alpha \simeq 0.5$) the flow separates if the Mach No. normal to the edge, \bar{M}_N , is subsonic, but is always attached if \bar{M}_N is supersonic.* \bar{M}_N is given in terms of mean edge sweepback $\bar{\Omega}$ and wing incidence α by

$$\bar{M}_N = \sqrt{M^2 \cos^2 \bar{\Omega} \cdot \cos^2 \alpha + M^2 \sin^2 \alpha} = \sqrt{M^2 \cos^2 \bar{\Omega} + M^2 \sin^2 \alpha \cdot \sin^2 \bar{\Omega}} \quad (10)$$

* There is some evidence that if $M\alpha > 0.6$, separated flow may persist up to low supersonic values of \bar{M}_N .

Clearly, then, the term $(b_u)_v$ will only appear in the case of slender wings with subsonic edges, (e.g. if $M > 2$, wings having an aspect ratio appreciably less than 2). For Mach Nos. not too near unity, it is reasonable to expect the value of $(b_u)_v$ to vary with \bar{M}_N , from about 4 at $\bar{M}_N = 0$ down to zero at $\bar{M}_N \approx 1.0$. Although \bar{M}_N is not necessarily the only parameter on which $(b_u)_v$ may depend - for example at Mach Nos. near unity $\beta \cot \bar{\Omega}$ and $\beta \alpha$ may also be important, nevertheless the empirical assumption is made that for a given type of edge $(b_u)_v$ depends mainly on \bar{M}_N . The strength of the vortex and hence the magnitude of $(b_u)_v$ is likely to be affected by the "sharpness" of the edge, i.e. by the wing thickness distribution in the region of the edges. This will be of particular importance in the case of very slender wings where a small wing depth in terms of chord has a large effect on the included angle at the leading edge near the wing apex. For these reasons, consideration is restricted in this survey to thin wings with sharp edges.

Experimental values⁵ of $(b_u)_v$ are plotted in Fig. 2 as a function of \bar{M}_N , the Mach Nos. normal to the mean swept edge. \bar{M}_N is given by equation (10) using the mean edge sweep $\bar{\Omega}$ of the line joining the leading edge of the centre-line chord to the trailing edge of the tip chord, (see sketches in Fig. 2). Using a mean edge sweep so defined, results for delta wings correlate reasonably well with those for wings with a curved leading edge or a finite tip chord. The values of $(b_u)_v$ have been derived from the slopes of lines drawn through experimental values of C_N/α plotted against α , due allowance being made for the effect of the hypersonic non-linear term (assuming $k = 0.7$) and the non-linear force on the lower surface (see section 3.1). For all the plotted points the mean C_N/α vs. α lines were drawn to cut the ordinate at $\alpha = 0$ at a value corresponding to the linear theory lift curve slope. The general trend of the points for $\alpha > 4^\circ$ supported this procedure in almost all cases, but C_N/α at $\alpha < 4^\circ$ tended to be below the lines so drawn.

It can be seen that the trend of the points in Fig. 2 is not inconsistent with the slender wing theory result $(b_u)_v \rightarrow 4$ for $\bar{M}_N \rightarrow 0$. However, no points are available on thin wings for $0 < \bar{M}_N < 0.3$ at supersonic stream Mach numbers, so in the absence of some guide to its shape, the curve in this range is shown broken.

At transonic speeds (say $1.0 < M < 1.2$) the conditions for the validity of slender wing theory may be satisfied although $\bar{M}_N \neq 0$. Under these conditions the curve of Fig. 2 would probably underestimate $(b_u)_v$. This is confirmed by the results of tests⁶ on a thick, $A = 1.2$ ogee wing, shown on Fig. 2, which gave values of $(b_u)_v$ well above the curve at $M = 1.0$ but broadly in agreement with it for $M = 1.25$.

2.3 Upper surface force as a function of Ma and Ma_u

In the foregoing it has been postulated that $(b_u)_v$ is a function of \bar{M}_N , which in turn depends on $M \cos \bar{\Omega}$ and $M \sin \alpha \sin \bar{\Omega}$, whereas the other upper surface non-linear force factor, $(b_u)_h$ depends on Ma and Ma_u .

It would obviously be very convenient if both $(b_u)_v$ and $(b_u)_h$, and hence b_u could be expressed solely in terms of Ma and Ma_u , since $M^2 C_{Nu}$ would then be a function of these two parameters by virtue of the relation

$$M^2 C_{Nu} = \frac{1}{2} Ma \cdot Ma_u + b_u (Ma_u)^2 \quad (11)$$

Now since $(b_u)_v$ is a factor most likely to be of importance in the case of slender wings, for which $\sin \bar{\Omega} \simeq 1$, it will usually be valid to make the approximation $M \sin \alpha \cdot \sin \bar{\Omega} \simeq Ma_u$. Again, the relation between $M \cos \bar{\Omega}$ and Ma for a delta wing of vanishingly small aspect ratio is a fair approximation to $M \cos \bar{\Omega}$ for a variety of low aspect ratio wings, as shown in Fig. 3. $M \cos \bar{\Omega}$ for a very slender delta is shown as a dashed line, and will be designated $(M \cos \bar{\Omega})_s$. Hence a new parameter $(\bar{M}_N)_s$ will be defined as follows, (cf equation (10)).

$$(\bar{M}_N)_s = \sqrt{(M \cos \bar{\Omega})_s^2 + (Ma_u)^2} \quad (12)$$

where $(\bar{M}_N)_s \simeq \bar{M}_N$ and is a function only of Ma and Ma_u .

All the experimental values of $(b_u)_v$ shown plotted against \bar{M}_N in Fig. 2 are plotted against $(\bar{M}_N)_s$ in Fig. 4. The mean line through these points is slightly different from that of Fig. 2, but the scatter about the line is much the same.

Finally, using equations (5), (6), (11), Fig. 4 and the theoretical relation between $(M \cos \bar{\Omega})_s$ and Ma shown on Fig. 3, Fig. 5 has been drawn showing $M^2 C_{Nu}$ as a function of Ma and Ma_u for thin, sharp edged wings at Mach. Nos. in excess of Mach 1.2. This picture makes clear the separate effects of $(b_u)_h$ and $(b_u)_v$.

It will be seen that for $Ma < 3$ there is a maximum in the C_{Nu} vs. α_u curve occurring at $Ma_u \simeq 0.7$, (i.e. at an incidence well below $\hat{\alpha}_u$) which is more pronounced the smaller the value of Ma . Since the curves for higher incidences depend critically on the shape of the Fig. 4 curve, - which is not well defined by the experimental data - the dashed parts of Fig. 5 should be regarded as tentative.

3 NORMAL FORCE ON LOWER SURFACE

In the prediction of normal force coefficient on the lower surface of thin wings, a distinction is made between wings which have substantial areas of two-dimensional flow with shocks attached to the leading edges (assumed sharp) up to a fairly large incidence, and those which do not come into this category. For clarity, an outline of the proposed method will first be made, showing how these two cases are dealt with, then details will be given in subsequent paragraphs.

Fig. 6 illustrates the proposed method for constructing the C_{Ne} vs. α_l curve. The curve labelled C_{Ne}' is essentially the "fully detached shock" case. It applies to wings with subsonic leading edges or with a shock detachment angle small enough to have a negligible influence on the shape of the C_{Ne} vs. α_l curve, and to any wing at an incidence about 30° above the shock detachment angle. Thus to sum up

$$C_{Ne} = C_{Ne}' \quad \text{if} \quad \alpha_l^* < 5^\circ$$

$$\text{or} \quad \alpha > \alpha_l^* + 30^\circ$$

Here, α_l^* is the lower surface incidence for shock detachment. Theoretical values of α_l^* for wings with plane lower surfaces, assuming a perfect gas with $\gamma = 1.4$, are shown in Fig. 7 as a function of Mach No. and leading edge sweep, Ω_0 . For the present analysis α_l^* will be assumed to be given by these theoretical results, surface curvature due to thickness being ignored.

If α_l^* is not too small and the tips do not influence each other the normal force coefficient will correspond with the upper curve in Fig. 6, which is the "shock-attached" case. This curve has two distinct phases. The first, $C_{Ne} = C_{Ne}^*$ extends up to $\alpha_l = \alpha_l^*$ and in this incidence range there is an attached leading edge shock with extensive two-dimensional flow on the wing. In the second phase the shock is detached but the normal force curve follows on from the first phase without discontinuity, and in this transition or "partially detached" phase $C_{Ne} = C_{Ne}' + \Delta C_{Ne}$. To sum up,

$$\text{If} \quad \alpha_l^* > 5^\circ \quad \underline{\text{and}} \quad \beta A > \frac{4\lambda}{1+\lambda}$$

$$C_{Ne} = C_{Ne}^* \quad \text{for} \quad \alpha_l < \alpha_l^*$$

$$C_{Ne} = C_{Ne}' + \Delta C_{Ne} \quad \text{for} \quad \alpha_l > \alpha_l^*$$

$$(\Delta C_{Ne} = 0 \quad \text{for} \quad \alpha_l > \alpha_l^* + 30^\circ)$$

The only remaining case is $\alpha_l^* > 5^\circ$ and βA less than $4\lambda/(1+\lambda)$. For this, interpolation between the attached and detached cases is suggested, proportional to $\beta A(1+\lambda)/4\lambda$.

In the following sections 3.1, 3.2 and 3.3, the estimation of C_{Ne}' and ΔC_{Ne} are discussed in turn.

3.1 Lower surface force with shock detached, C_{Ne}'

It is proposed to base the estimation of C_{Ne}' on theoretical results strictly applicable to slender wings. Munk has shown⁷ that in inviscid flow the normal force on a slender wing or body is proportional to the product of the axial and transverse velocity components, i.e. it varies as $\sin\alpha \cos\alpha$. Hence considering the lower surface only, there will be a normal force coefficient $\frac{a}{2} \sin\alpha \cos\alpha$ due to the action in combination of axial and transverse velocities, and an additional force due to the transverse velocity alone. Remembering that the transverse flow is two-dimensional in the case of a slender wing or body, this additional force must be equal to that on the lower surface of the wing or body at 90° incidence in a stream of speed $V \sin\alpha$ and Mach No. $M \sin\alpha$; (pressure measurements on inclined infinite cylinders, for which $a = 0$, confirm this). Thus for a slender wing we can write

$$(C_{Ne})_s = \frac{a}{2} \sin\alpha_\ell \cos\alpha_\ell + (b_\ell)_s \sin^2 \alpha_\ell \quad (13)$$

where $(b_\ell)_s$ is the lower surface normal force coefficient on the wing at 90° incidence at a stream Mach No. $M \sin\alpha_\ell$. It may be noted that if $M \sin\alpha_\ell > 1$ there will be a shock parallel with the lower surface to which the transverse flow Mach No. $M \sin\alpha_\ell$ is normal.

For non-slender wings which yet have detached leading edge shocks the flow picture is exceedingly complex and there is no simple theoretical basis for the estimation of C_{Ne}' . In the absence of an equally simple alternative it is proposed to retain the general form of equation (13) and to regard the first term as applicable to all wings in this category. However, in the general case the transverse flow factor b_ℓ is likely to differ from that for slender wings $(b_\ell)_s$ if only because the mean inclination to the stream of the detached shock will be less and the effective Mach No. for the transverse flow will lie somewhere between the slender wing value, $M \sin\alpha_\ell$ and the maximum value which is of course the stream Mach No. M . The latter will probably apply to the case of an unswept wing of high aspect ratio with detached shock because the flow affecting the lower surface passes almost normally through the shock. In order to take account of these considerations, albeit crudely, it will be assumed that b_ℓ is a function of \bar{M}_N , the Mach number normal to the mean leading edge (equation 10) which tends to the required limits for both slender wings and unswept wings.

$$C_{Ne}' = \frac{a}{2} \sin\alpha_\ell \cos\alpha_\ell + b_\ell \sin^2 \alpha_\ell \quad (14)$$

where b_ℓ , the transverse flow factor is the lower surface normal force coefficient at 90° incidence in a stream of Mach No. \bar{M}_N , where the latter is given by equation (10) with $\alpha = \alpha_\ell$.

Experimental values⁹ of b_ℓ are shown on Fig. 8 for both flat circular plates and flat two-dimensional strips. On this evidence there seems to be no significant, consistent difference between these two extreme cases, so b_ℓ will be assumed to be independent of planform. Also shown on this Fig. for $\bar{M}_N > 1$ is the theoretical curve of b_ℓ for circular plates obtained by Maccoll and Codd¹⁰, and since this curve fits the experimental data reasonably well it is proposed to use these theoretical values of b_ℓ in equation (14).

The result obtained by Maccoll and Codd is

$$b_\ell = 0.9054 C_{p_s} - \frac{0.1892}{\gamma \bar{M}_N^2} \quad (15)$$

where C_{p_s} is the pitot pressure coefficient, shown on Fig. 8 for $\gamma = 1.4$, corresponding to the effective normal Mach No. \bar{M}_N . To complete the picture, the trend of experimental results¹¹ for b_ℓ at subsonic normal Mach Nos. up to 0.8 is also given, and a plausible line joining these to the supersonic theoretical curve can readily be drawn as shown.

3.2 Lower surface force with shock attached $C_{N\ell}$

If there is a shock attached to the leading edge and at the same time the angle of incidence is great enough for non-linearities in the normal force curve to be appreciable, the Mach angle ($\sin^{-1} 1/M$) will in most cases be small enough to ensure that the flow over the larger part of the wing will be two-dimensional. Accordingly it is proposed that the normal force coefficient $C_{N\ell}$ be estimated by modifying theoretical values of the pressure coefficient on a two-dimensional wedge of semi-angle α_ℓ to allow for three-dimensional tip effects. Those wings which have interfering tips are excluded so that the conditions for the following method to apply are

$$\begin{aligned} \alpha_\ell &< \alpha_\ell^* \\ \beta A &> \frac{4\lambda}{1+\lambda} \quad . \end{aligned}$$

There are two semi-empirical methods for estimating $C_{N\ell}$, both of which give good agreement with experiment if the above conditions are fulfilled.

(a) The first is to use the oblique shock equations or tabulated solutions thereof to obtain $(C_{N\ell}^x)_{2D}$, the two-dimensional value of $C_{N\ell}^x$, and correct this by assuming linear theory tip losses, i.e.

$$C_{N\ell}^x = (C_{N\ell}^x)_{2D} - \left(\frac{2}{\beta} - \frac{a}{2}\right) \alpha_\ell \quad (16)$$

where a is of course the wing lift slope according to linearised theory.

(b) A more convenient and no less accurate method is to use a modified form of the so called strong shock approximation^{12,14}. By assuming M large and α_ℓ small the following expression for $(C_{N\ell}^x)_{2D}$ can be derived from the oblique shock equations

$$\frac{(C_{N\ell}^x)_{2D}}{\alpha_\ell^2} \quad \text{for} \quad \begin{matrix} M \rightarrow \infty \\ \alpha_\ell \rightarrow 0 \end{matrix} = \frac{\gamma+1}{2} + \sqrt{\frac{4}{(M\alpha_\ell)^2} + \left(\frac{\gamma+1}{2}\right)^2} \quad (17)$$

This expression can be empirically modified to extend its range of applicability, first to lower Mach Nos. and larger angles, second to finite wings, as follows.

(i) The first term on the right hand side, $(\gamma+1)/2$ is replaced by the analogous coefficient of α_ℓ^2 in the Busemann expansion¹³ for $(C_{N\ell}^x)_{2D}$. In effect, this means adding a term $(B)_{2D} = f(M)$ to the right hand side of the equation, where

$$(B)_{2D} = \frac{\gamma-1}{\beta^2} + \frac{\gamma+1}{2\beta^4} \quad (18)$$

This term is negligible for $M > 3$.

(ii) The dependent variable $(C_{N\ell}^x)_{2D}/\alpha_\ell^2$ is replaced by the impact theory¹⁴ equivalent $(C_{N\ell}^x)_{2D}/\sin^2\alpha_\ell$, thus giving the correct limit for $M\alpha_\ell \rightarrow \infty$.

(iii) The small angle hypersonic similarity parameter $M\alpha_\ell$ is replaced by a large angle, supersonic-hypersonic equivalent $\beta \sin\alpha_\ell \cos\alpha_\ell$. The substitution of β for M follows Van Dyke's supersonic-hypersonic similarity rule¹⁵, but the substitution of $\sin\alpha_\ell \cos\alpha_\ell$ for α_ℓ is an empirical change justified by the very good correlations of exact solutions for both wedges and cones which are thereby obtained. The resulting expression for $(C_{N\ell}^x)_{2D}$ is then

$$\frac{(C_{N\ell}^x)_{2D}}{\sin^2\alpha_\ell} = \frac{\gamma+1}{2} + (B)_{2D} + \sqrt{\frac{4}{(\beta \sin\alpha_\ell \cos\alpha_\ell)^2} + \left(\frac{\gamma+1}{2}\right)^2} \quad (19)$$

Fig. 9 shows the ratio of $(C_{N\ell})_{2D}$ estimated by means of equations (18) and (19) to $(C_{N\ell})_{2D}$ obtained from solutions of the oblique shock equations, with $\gamma = 1.4$. The difference between the two methods is not greater than 5% for angles of incidence up to about 4° below that for shock detachment, and is within 2% for angles up to about 8° below that for shock detachment. These differences are of little practical significance, since thickness and viscosity effects cause the actual lower surface force coefficients to fall below the theoretical values at angles of incidence just below α_ℓ^* .

(iv) Finally, for three-dimensional wings the "two-dimensional" variable $\beta \sin \alpha_\ell \cos \alpha_\ell$ is replaced by its "three-dimensional" equivalent, $\frac{4}{a} \sin \alpha_\ell \cos \alpha_\ell$,

$$\frac{C_{N\ell}}{\sin^2 \alpha_\ell} = \frac{\gamma+1}{2} + B + \sqrt{\left(\frac{a}{2 \sin \alpha_\ell \cos \alpha_\ell}\right)^2 + \left(\frac{\gamma+1}{2}\right)^2}$$

It may be noted that at Mach. Nos. great enough for B to be negligible, i.e. $M > 3$, the above expression is consistent with the small angle supersonic-hypersonic similarity rule¹⁵, $C_{N\ell}/\alpha_\ell^2 = f(\beta \alpha_\ell, \beta A)$, since for 'similar' wings $\beta a = f(\beta A)$.

The low Mach No. correction term B is a function of β and is probably affected by tip losses. On the evidence of experimental data, the empirical assumption is made that B is proportional to a. The final expression for $C_{N\ell}$ rearranged in a form suitable for graphical presentation is

$$\frac{C_{N\ell}}{a \tan \alpha_\ell} - \frac{B}{a} \sin \alpha_\ell \cos \alpha_\ell = \frac{\gamma+1}{2} \left(\frac{\sin \alpha_\ell \cos \alpha_\ell}{a}\right) + \frac{1}{2} \sqrt{1 + \left[(\gamma+1) \left(\frac{\sin \alpha_\ell \cos \alpha_\ell}{a}\right)\right]^2}$$

..... (20)

where

$$\frac{B}{a} = \frac{\gamma-1}{4\beta} + \frac{\gamma+1}{8\beta^3} \quad (21)$$

A chart for the estimation of $C_{N\ell}$ based on this equation with $\gamma = 1.4$ is given on Fig. 10.

3.3 Lower surface force with shock 'partially attached', $C_{N\ell}^i + \Delta C_{N\ell}$

Although the leading edge shock is, strictly speaking, detached if $\alpha_\ell > \alpha_\ell^*$, the lower surface normal force does not fall to the value appropriate to the fully detached shock case (equation 14) until $\alpha_\ell > \alpha_\ell^* + 30^\circ$. In the range $\alpha_\ell^* < \alpha_\ell < \alpha_\ell^* + 30^\circ$ the shock can be regarded

as 'partially detached' and the lower surface normal force coefficient exceeds C_{Ne}' by ΔC_{Ne} , i.e.

$$C_{Ne} = C_{Ne}' + \Delta C_{Ne} \quad \text{for } \alpha_\ell^* < \alpha_\ell < \alpha_\ell^* + 30^\circ \quad (22)$$

A curve for estimating ΔC_{Ne} , derived purely from experimental data, is given in Fig. 11. ΔC_{Ne} is expressed in terms of $\alpha_\ell - \alpha_\ell^*$, ΔC_{Ne}^* and θ^* . ΔC_{Ne}^* is the difference between C_{Ne} and C_{Ne}' at $\alpha_\ell = \alpha_\ell^*$ while θ^* is the difference between $dC_{Ne}/d\alpha_\ell$ and $dC_{Ne}'/d\alpha_\ell$ at $\alpha_\ell = \alpha_\ell^*$. The form of the curve of ΔC_{Ne} is prescribed by the assumed condition that there should be no discontinuity in $dC_{Ne}/d\alpha_\ell$ through α_ℓ^* .

Direct experimental support for this curve is not given in the figure because owing to the small quantities involved there is inevitably a lot of scatter. The effectiveness of the method for predicting C_{Ne} for $\alpha_\ell > \alpha_\ell^*$ can better be judged from the comparisons between measured and estimated C_N described in the following section and on Fig. 13. On the latter the estimate of total C_N assuming a fully detached leading-edge shock, $C_{Nu} + C_{Ne}'$ is shown as a dashed line, the difference between this and the actual estimate in each case, shown as a full line, being ΔC_{Ne} for $\alpha_\ell > \alpha_\ell^*$.

4 COMPARISONS BETWEEN ESTIMATED AND MEASURED NORMAL FORCE

Estimates of normal force coefficient based on the foregoing method have been made for a number of thin wings, (thickness/chord $< 5\%$), for which measured values are available to fairly high angles of incidence. These comparisons are presented graphically, in Figs. 12 for the shock detached cases and in Fig. 13 for shock attached cases.

All estimates shown as full lines in these figures have been made with the following assumptions

- (i) Initial force curve slope, a , as given by linearised theory.
- (ii) $k = 0.7$ and $(b_u)_v = f(\bar{M}_N)$, i.e. C_{Nu} given in Fig. 5.

The contribution of C_{Nu} to C_N is shown for each comparison, and in the case of wings having $\alpha_\ell^* > 5^\circ$, the 'shock detached' estimate, $C_{Nu} + C_{Ne}'$.

In Fig. 12 measured values of C_N on delta wings are compared with estimates, all these cases being 'shock detached'. The full lines show the estimates of C_N , while the dotted lines assumes $b_\ell = f(M \sin \alpha)$ instead of $f(\bar{M}_N)$, (i.e. the slender wing case). These results do not allow a choice to be made between the two methods, the difference between them being small, and the agreement of theory with experiment being good in each case.

Figs. 13(a), (13(b), 13(c) compare measured and estimated C_N for various wings in the 'shock-attached' category, i.e. $\alpha_\ell^* > 5^\circ$. Fig. 13(a) deals with rectangular wings with $\beta A > 2$, i.e. tips which do not interfere. The agreement in these cases is good in general, the least satisfactory correlation being the aspect ratio 1 wing at Mach 6.85 (Ref. 20) at incidences greater than 40° ; this wing however had rounded edges, which may account partially for the discrepancy. Fig. 13(b) shows two rectangular wings having interfering tips, i.e. with $\beta A < 2$; in these cases the estimates are interpolations between the shock detached and shock attached values. The $A = 1$ wing at Mach 1.45 has an appreciable leading edge vortex contribution to normal force, as shown. Lastly, Fig. 13(c) compares results for delta wings having $\alpha_\ell^* > 5^\circ$, which tend, of course, to be at higher Mach. Nos.

Perhaps the most striking feature of these results is the relatively small contribution to normal force from the upper surface at high angles if the Mach No. exceeds about 3.

5 SUMMARY OF METHOD

It will be assumed that the initial force curve slope is known, and the problem is to estimate the non-linear force. The normal force coefficient C_N on a thin wing with sharp edges at supersonic speeds ($M > 1.25$) may then be estimated from the following summary, in conjunction with the list of symbols

$$C_N = C_{Nu} + C_{N\ell} \quad (1)$$

where C_{Nu} is given by Fig. 5 as a function of M , $M\alpha_u$ and $M\alpha$. Obtain α_ℓ^* from Fig. 7.

If $\alpha_\ell^* < 5^\circ$

$$C_{N\ell} = C_{N\ell}' = \frac{a}{2} \sin \alpha_\ell \cos \alpha_\ell + b_\ell \sin^2 \alpha_\ell \quad (14)$$

where b_ℓ is given by Fig. 8 as a function of $\bar{M}_N = M \sqrt{\cos^2 \bar{\Omega} \cos^2 \alpha_\ell + \sin^2 \alpha_\ell}$.

If $\alpha_\ell^* > 5^\circ$ and $\beta A > \frac{4\lambda}{1+\lambda}$

$$C_{N\ell} = C_{N\ell}^\times \text{ given by Fig. 10 for } \alpha_\ell < \alpha_\ell^*$$

$$C_{N\ell} = C_{N\ell}^i + \Delta C_{N\ell} \text{ for } \alpha_\ell > \alpha_\ell^*$$

where $\Delta C_{N\ell}$ is given by Fig. 11.

If $\alpha_\ell^* > 5^\circ$ and $\beta A < \frac{4\lambda}{1+\lambda}$

$C_{N\ell}$ interpolated between $C_{N\ell}^i$ and the estimate for $\beta A > \frac{4\lambda}{1+\lambda}$,
in proportion to $\beta A(1+\lambda)/4\lambda$.

6 CONCLUSIONS

A simple semi-empirical method has been devised for the prediction of non-linear normal force on thin wings with sharp edges, which is compatible with relevant theoretical and experimental results at angles of incidence up to 90° .

An extension of this analysis is desirable to include effects of thickness, which are thought to be particularly important in the case of slender wings.

Experimental confirmation is required of an implication of the proposed method that there is a pronounced double maximum in the upper surface normal force vs. incidence curve if Mach No. \times lift curve slope is less than about 2.

LIST OF SYMBOLS

a	initial force curve slope, $(dC_N/d\alpha)_{\alpha \rightarrow 0}$
b_u, b_ℓ	non-linear force factors, associated with upper and lower surfaces respectively
$(b_u)_h$	component of b_u associated with hypersonic parameter $M\alpha$ (see section 2.1)
$(b_u)_v$	component of b_u associated with leading edge vortices (see section 2.2)
\bar{c}	mean chord
\bar{d}	mean thickness at trailing edge
k	ratio $\hat{C}_{Nu}/(-C_p)_{\text{vac}}$

LIST OF SYMBOLS (Contd)

A	aspect ratio
B	function of a and M , given by equation (21)
C_N	normal force coefficient, normal force $+ \frac{1}{2} V^2 S$
C_{Ne}	part of normal force coefficient contributed by lower surface
C_{Ne}^*	C_{Ne} with attached leading edge shock (see Fig. 6)
$C_{Ne}^!$	C_{Ne} with detached leading edge shock (see Fig. 6)
ΔC_{Ne}	$C_{Ne} - C_{Ne}^!$ for $\alpha_\ell^* < \alpha_\ell < \alpha_\ell^* + 30^\circ$ (see Fig. 6)
C_{Nu}	part of normal force coefficient contributed by upper surface
\hat{C}_{Nu}	maximum value of $C_{Nu} = f(\alpha_u)$
C_p	pressure coefficient, (local pressure - stream static pressure) $+ \frac{1}{2} \rho V^2$
$(-C_p)_{\max}$	maximum negative pressure coefficient
$(-\bar{C}_p)_t$	mean negative pressure coefficient due to thickness
C_{ps}	pitot pressure coefficient
$(-C_p)_{\text{vac}}$	negative pressure coefficient corresponding to absolute vacuum, $= 2/\gamma M^2$
M	stream Mach No.
\bar{M}_N	Mach No. normal to mean edge, (see Fig. 2)
$(\bar{M}_N)_s$	approximation to \bar{M}_N in terms of Ma and Ma_u (see Figs. 3 and 4)
S	wing plan area
V	stream velocity
α	incidence of chord line
α_u, α_ℓ	incidence of upper and lower surfaces respectively, see equation (2)
$\hat{\alpha}_u$	value of α_u at which \hat{C}_{Nu} is first attained
β	$\sqrt{M^2 - 1}$
γ	ratio of specific heats, assumed to be 1.4

LIST OF SYMBOLS (Contd)

θ^*	$dC_{N\ell}^x/d\alpha_\ell = dC_{N\ell}^i/d\alpha_\ell$ at $\alpha_\ell = \alpha_\ell^*$
λ	ratio, tip chord/root chord
Ω_0	sweepback of leading edge
$\bar{\Omega}$	mean edge sweepback, that of line joining root L.E. to tip T.E.
ρ	stream density
[] _{2D}	in two-dimensional flow
[] _s	applying to slender wings
[]*	at shock detachment

LIST OF REFERENCES

<u>No.</u>	<u>Author</u>	<u>Title etc.</u>
1	Relf, E.F.	Note on the maximum attainable suction on a body in an air stream. ARC 16062 July, 1953
2	Mayer, J.P.	A limit pressure coefficient and an estimation of limit forces on airfoils at supersonic speeds. NACA RM 18F23 TIB/1892 August, 1948
3	Mangler, K.W. Smith, J.H.B.	Calculation of the flow past slender delta wings with leading edge separation. Proc. Roy. Soc. Series A, Vol. 251, pp. 200-217, 1959.
4	Stanbrook, A. Squire, L.C.	Possible types of flow at swept leading edges. ARC 21,464 April 1959
5	Igglesden, M.S.	Tabulated lift, drag and pitching moment data from wind tunnel tests on 30 slender wings of ogee and other planforms, with various thickness distributions at $M = 1.41, 1.61$ and 1.91 . ARC 22,709. November 1960.
6	Squire, L.C. Capps, D.S.	Experimental investigation of the characteristics of an ogee wing from $M = 0.4$ to $M = 1.8$. ARC C.P. 585. August, 1959.

LIST OF REFERENCES (Contd)

<u>No.</u>	<u>Author</u>	<u>Title</u>
7	Munk, M.M.	Fluid Mechanics Part II, section C of "Aerodynamic Theory", Editor W.F. Durand Pub. Julius Springer, 1934
8	Penland, J.A.	Aerodynamic characteristics of a circular cylinder at Mach. No. 6.86 and angles of attack up to 90°. NACA TN 3861, January, 1957.
9	-	Handbook of Supersonic Aerodynamic Data Section 5.1.1. Fig. 4 December, 1957
10	Maccoll, J.W. Codd, J.	Theoretical investigations of the flow around various bodies in the sonic region of velocities. ARC 9315 September, 1945
11	Hoerner, S.F.	Fluid-dynamic drag 1958
12	Lees, Lester	Hypersonic flow Fifth International Aeronautical Conference, 1955
13	-	Handbook of Supersonic Aerodynamic Data Section 0.3.2. February, 1956
14	Crabtree, Dr. L.F.	Survey of inviscid hypersonic flow theory for geometrically slender shapes. RAE Tech. Note No. Aero 2695 June, 1960
15	Van Dyke, M.	Combined hypersonic-supersonic similarity rule. Journal of Aero Sciences July, 1951
16	Gallagher, J.J. Mueller, J.N.	An investigation of the maximum lift of wings at supersonic speeds. NACA Report 1227 1955
17	Hill, W.A.	Experimental lift of low aspect ratio triangular wings at large angles of attack and supersonic speeds. NACA RM A57I17 TIL/5765 November, 1957
18	Kaattari, G.E.	Pressure distributions on triangular and rectangular wings to high angles of attack - Mach. Nos. 2.46 and 3.36. NACA RM A54J12 TIL/4532 January, 1955
19	Bertram, M.H. McCauley, W.D.	An investigation of the aerodynamic characteristics of thin delta wings with a symmetrical double-wedge section at a Mach No. of 6.9. NACA RM L55B14 TIL/4654 April, 1955
20	Penland, J.A. Armstrong, W.O.	Static longitudinal aerodynamic characteristics of several wing and blunt-body shapes applicable for use as re-entry configurations at a Mach.No. of 6.8 and angles of attack up to 90°. NASA TM X-65 October, 1959

LIST OF REFERENCES (Contd)

<u>No.</u>	<u>Author</u>	<u>Title etc.</u>
21	Pitts, W.C.	Force, moment and pressure-distribution characteristics of rectangular wings at high angles of attack and supersonic speeds. NACA RM A55K09 TIL/4972 February, 1956
22	McLellan, C.H. Bertram, M.H. Moore, J.A.	An investigation of four wings of square planform at a Mach No. of 6.9 in the Langley 11 inch hypersonic tunnel. NACA Report 1310 1957

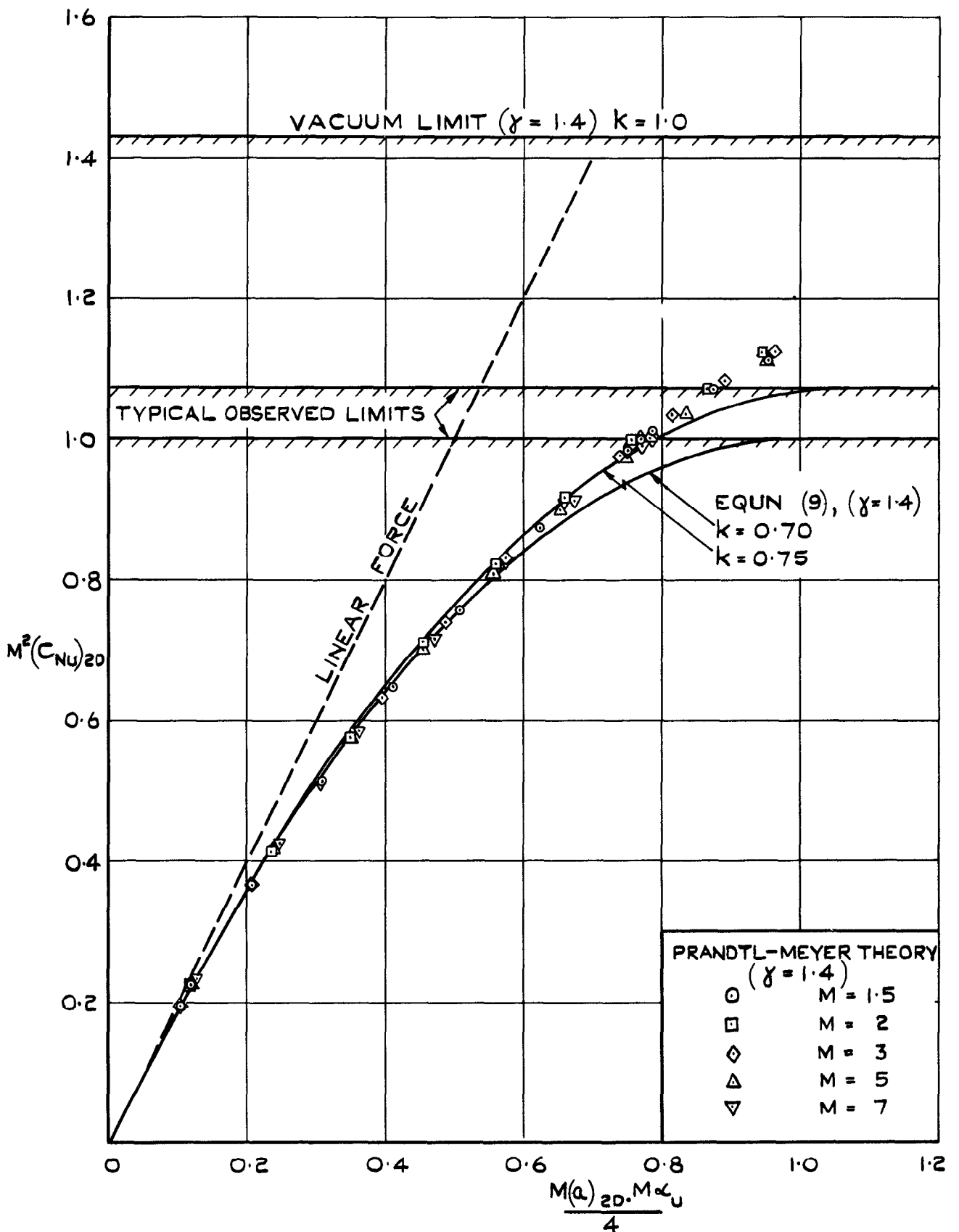


FIG. I. NORMAL FORCE ON UPPER SURFACE OF FLAT PLATE IN TWO-DIMENSIONAL FLOW.

SYMBOL	△	△	△	⊙	⊙	⊙
PLANFORM	DELTA			GOTHIC		
ASPECT RATIO	3/4	1	4/3	3/4	1	4/3
MACH NO	1.41, 1.61 & 1.91					
RANGE OF Mα	0.15-0.3					
REFERENCE	5					

TAGS ON SYMBOLS REFER TO VALUES OBTAINED AT NEGATIVE ANGLES OF INCIDENCE

NOTES: (i) $(b_u)_v$ DERIVED FROM MEASURED C_N AND EQUATIONS 1,3,5,6,14 ASSUMING $k=0.7$ AND $\alpha = \text{LINEAR THEORY LIFT SLOPE}$

$$(ii) \bar{M}_N = \sqrt{M^2 \cos^2 \bar{\Lambda} + M^2 \sin^2 \alpha \cdot \sin^2 \bar{\Lambda}}$$

(iii) MEAN EDGE SWEEP $\bar{\Lambda}$ DEFINED AS BELOW

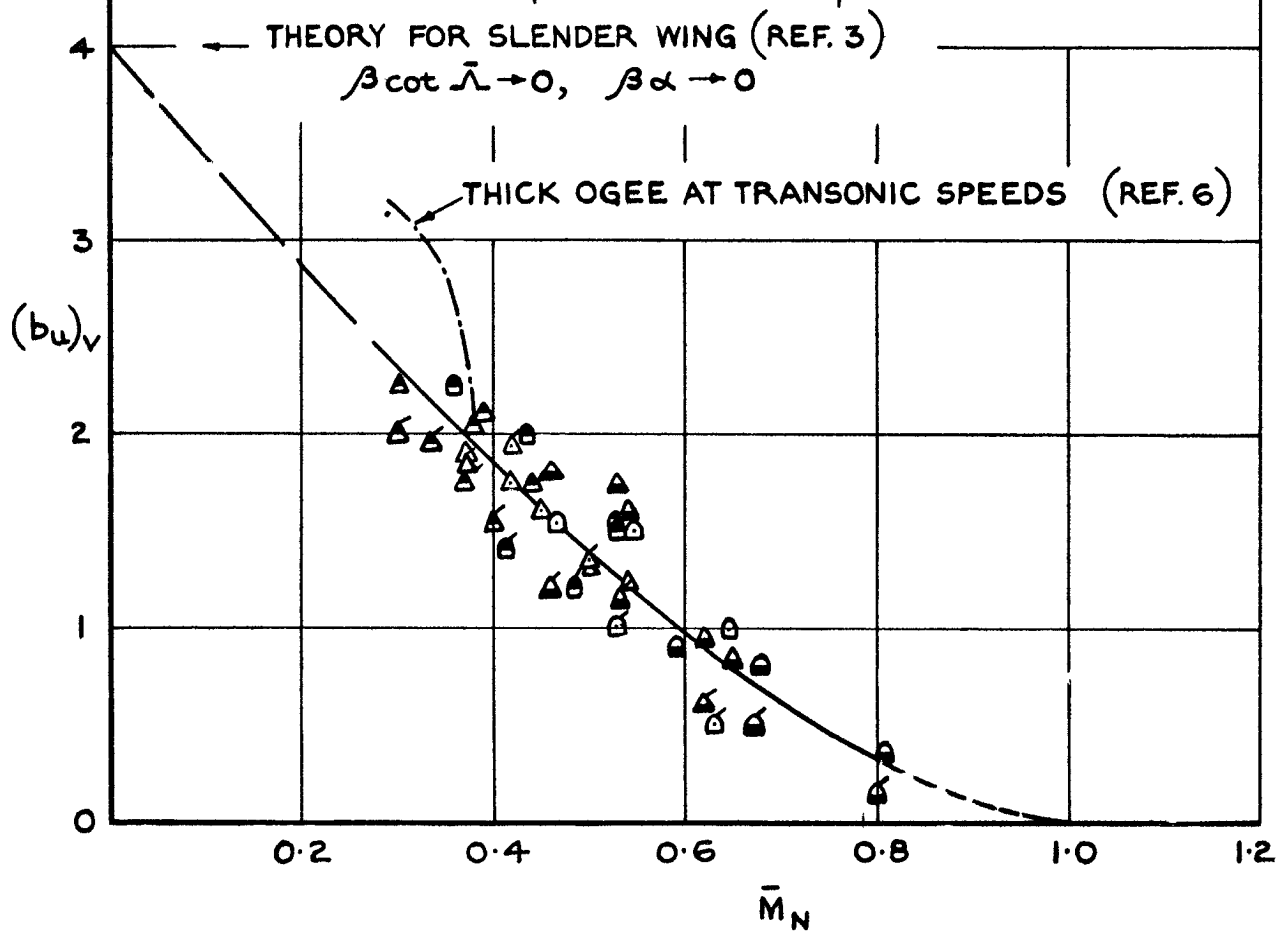


FIG.2. THE LEADING EDGE VORTEX NORMAL FORCE FACTOR $(b_u)_v$ AS A FUNCTION OF MACH NO NORMAL TO MEAN SWEPT EDGE, FOR THIN, SHARP-EDGED WINGS AT SUPERSONIC SPEEDS.

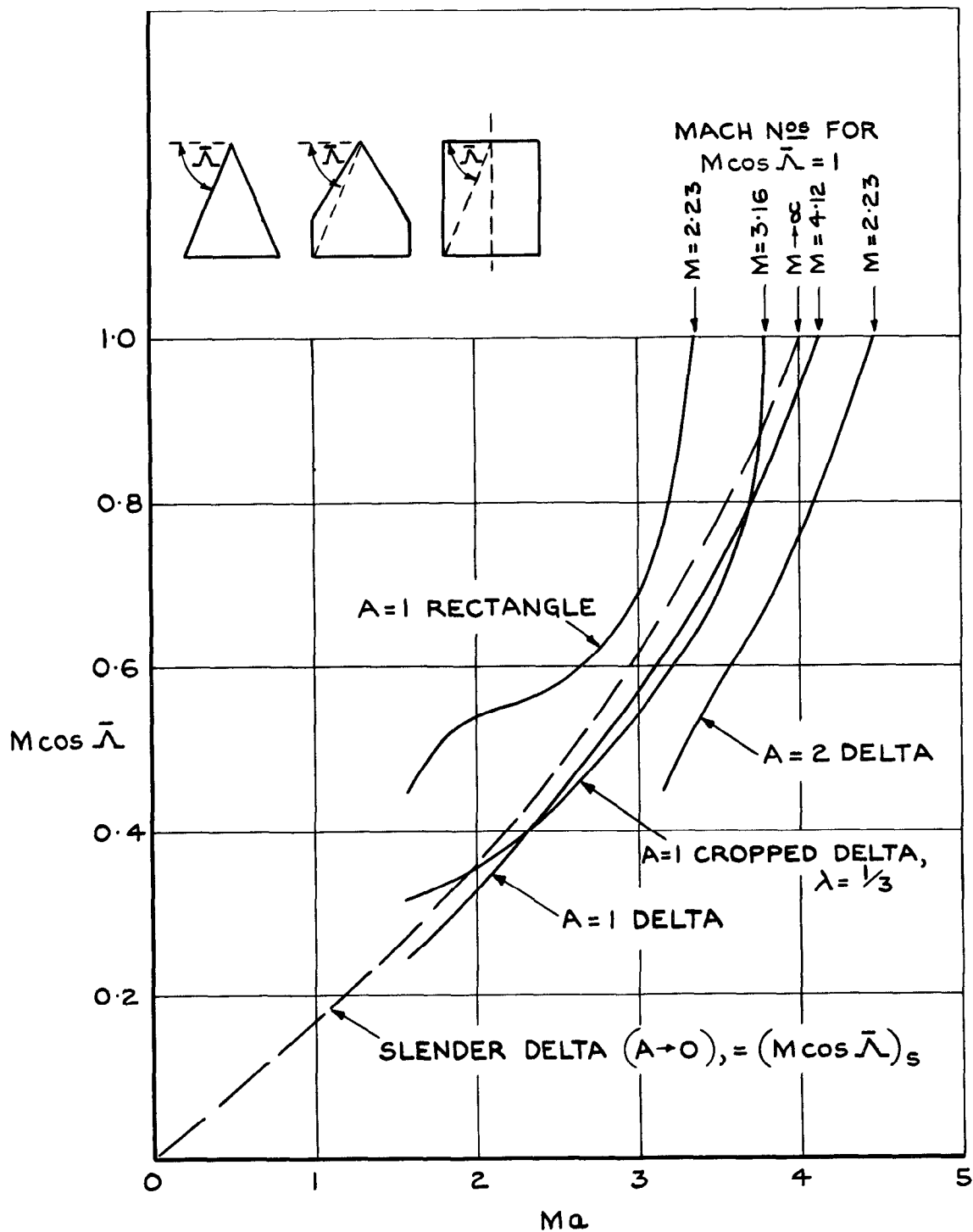


FIG.3. MACH NO NORMAL TO MEAN SWEEP EDGE AT ZERO INCIDENCE, AS A FUNCTION OF Ma , FOR VARIOUS SLENDER WINGS.

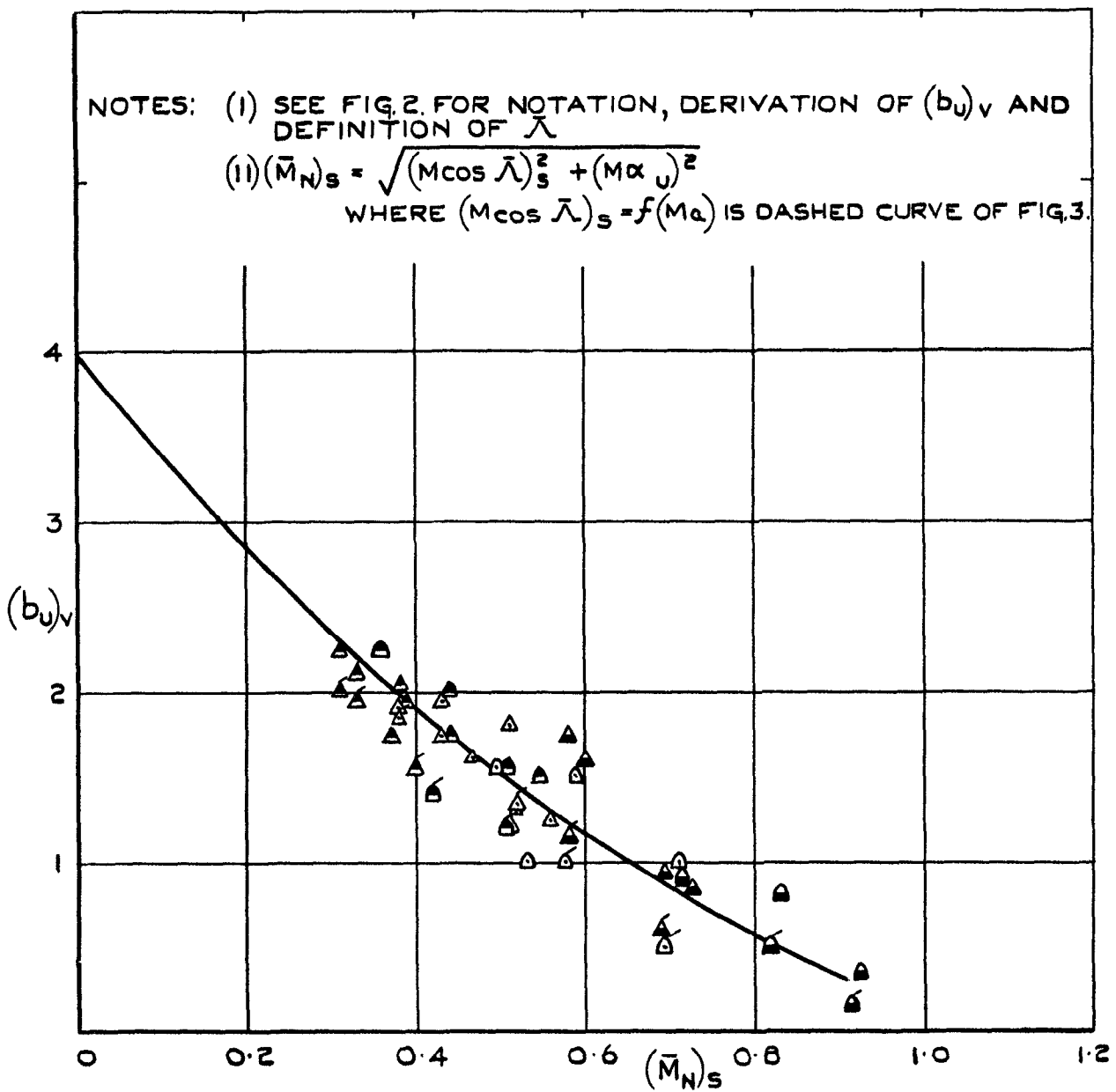


FIG. 4. THE LEADING-EDGE VORTEX NORMAL FORCE FACTOR $(b_u)_v$ AS A FUNCTION OF M_α & $M \alpha_u$, FOR THIN, SHARP-EDGED WINGS AT SUPERSONIC SPEEDS.

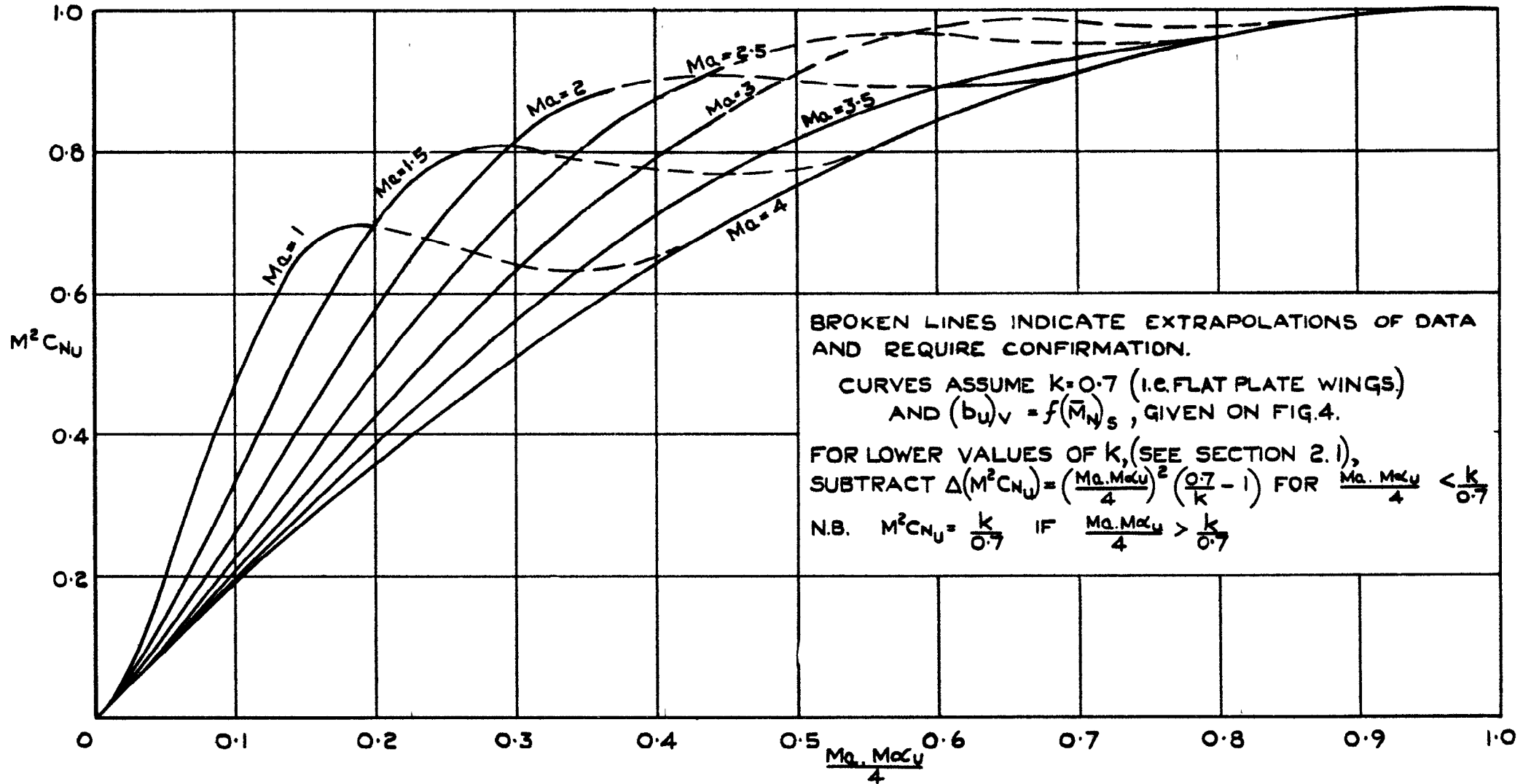


FIG. 5. NORMAL FORCE ON UPPER SURFACE OF THIN, SHARP-EDGED WINGS AT SUPERSONIC SPEEDS, AS A FUNCTION OF M_{∞} AND $M_{\infty U}$.

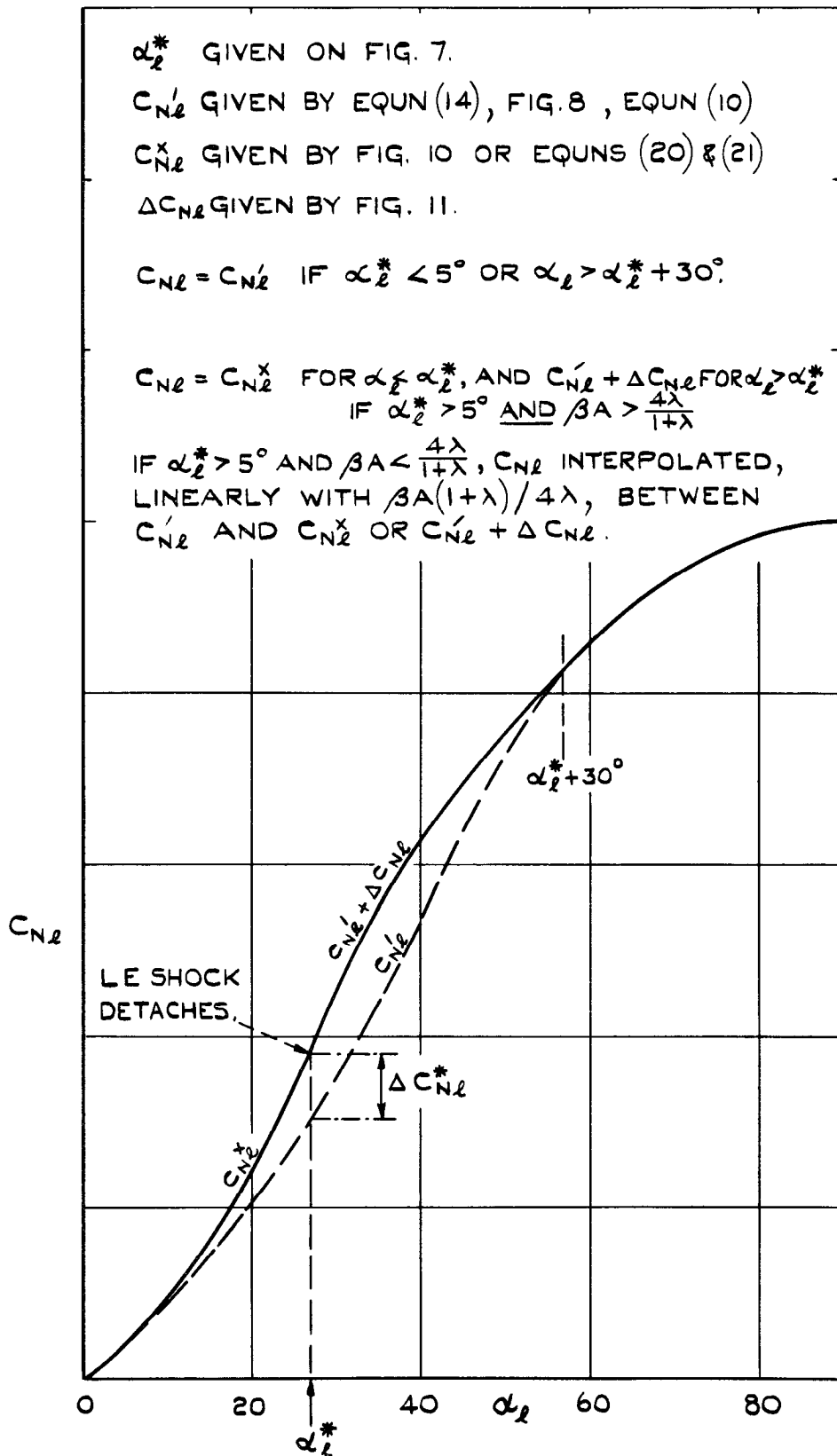


FIG.6. CONSTRUCTION OF C_{N2} vs α_2 CURVE.

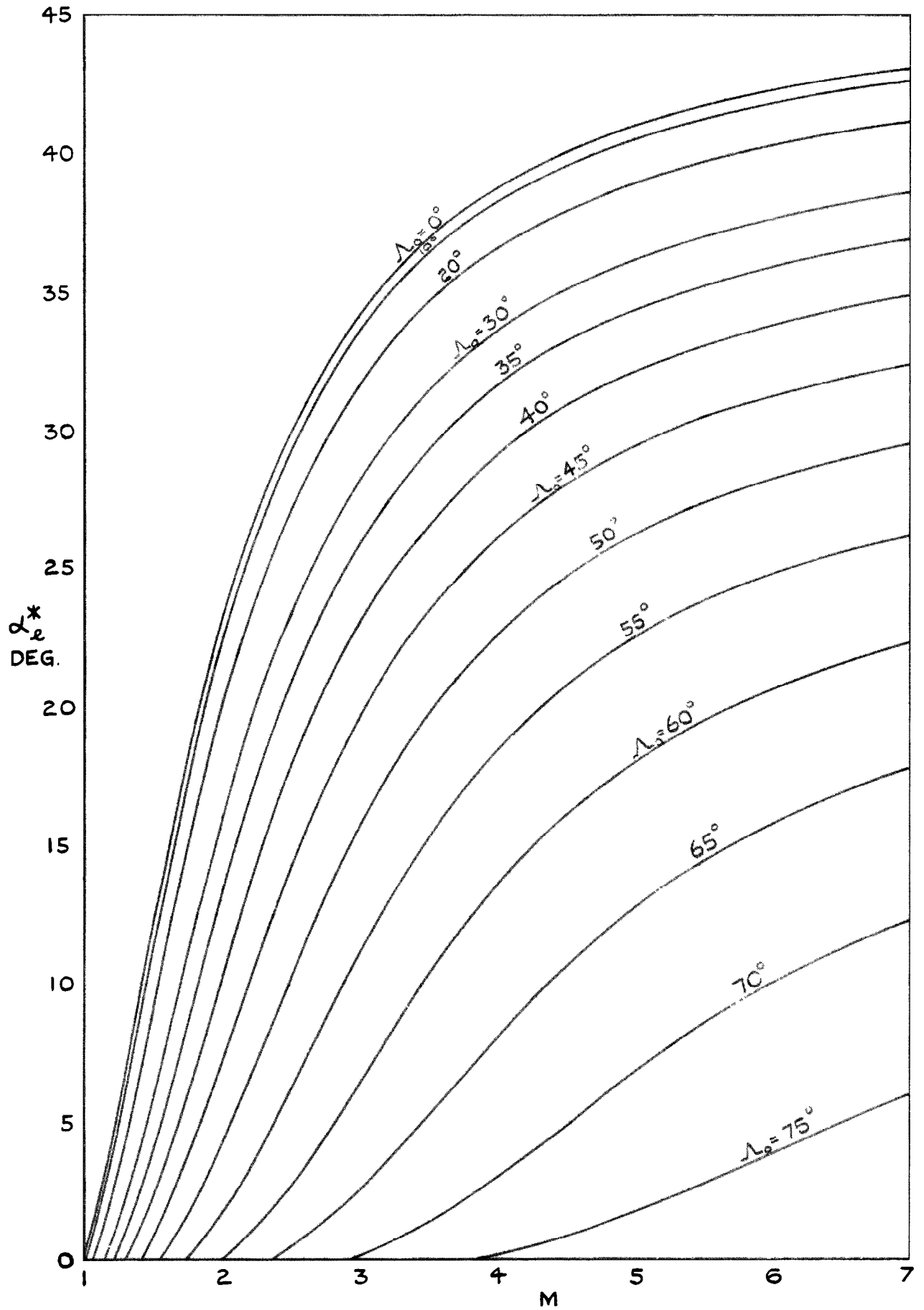


FIG.7. LOWER SURFACE INCIDENCE FOR SHOCK DETACHMENT α_l^* , FOR THIN, SHARP-EDGED WINGS.

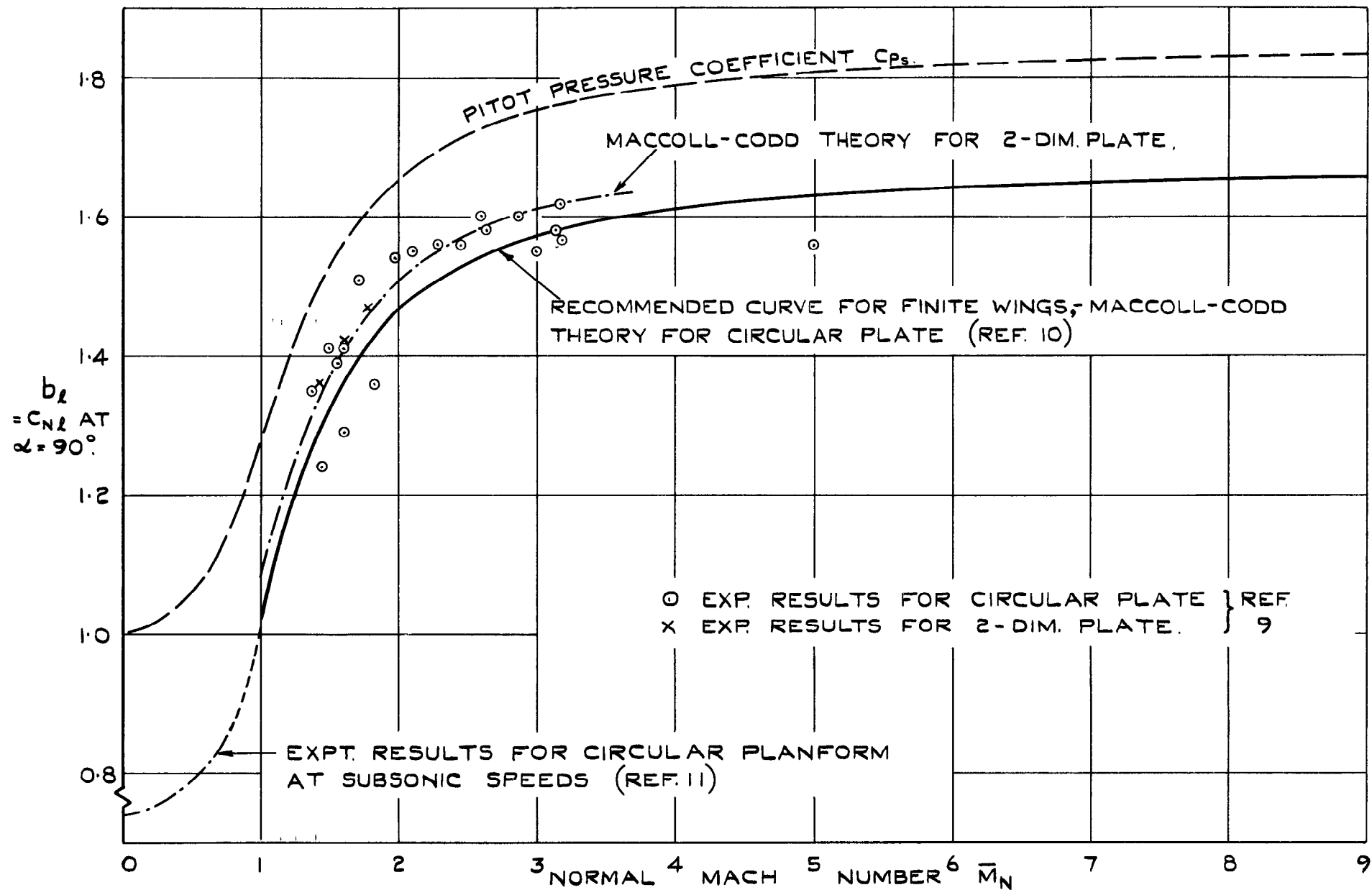


FIG. 8. NORMAL FORCE COEFFICIENT ON LOWER SURFACE OF THIN WINGS AT 90° INCIDENCE.

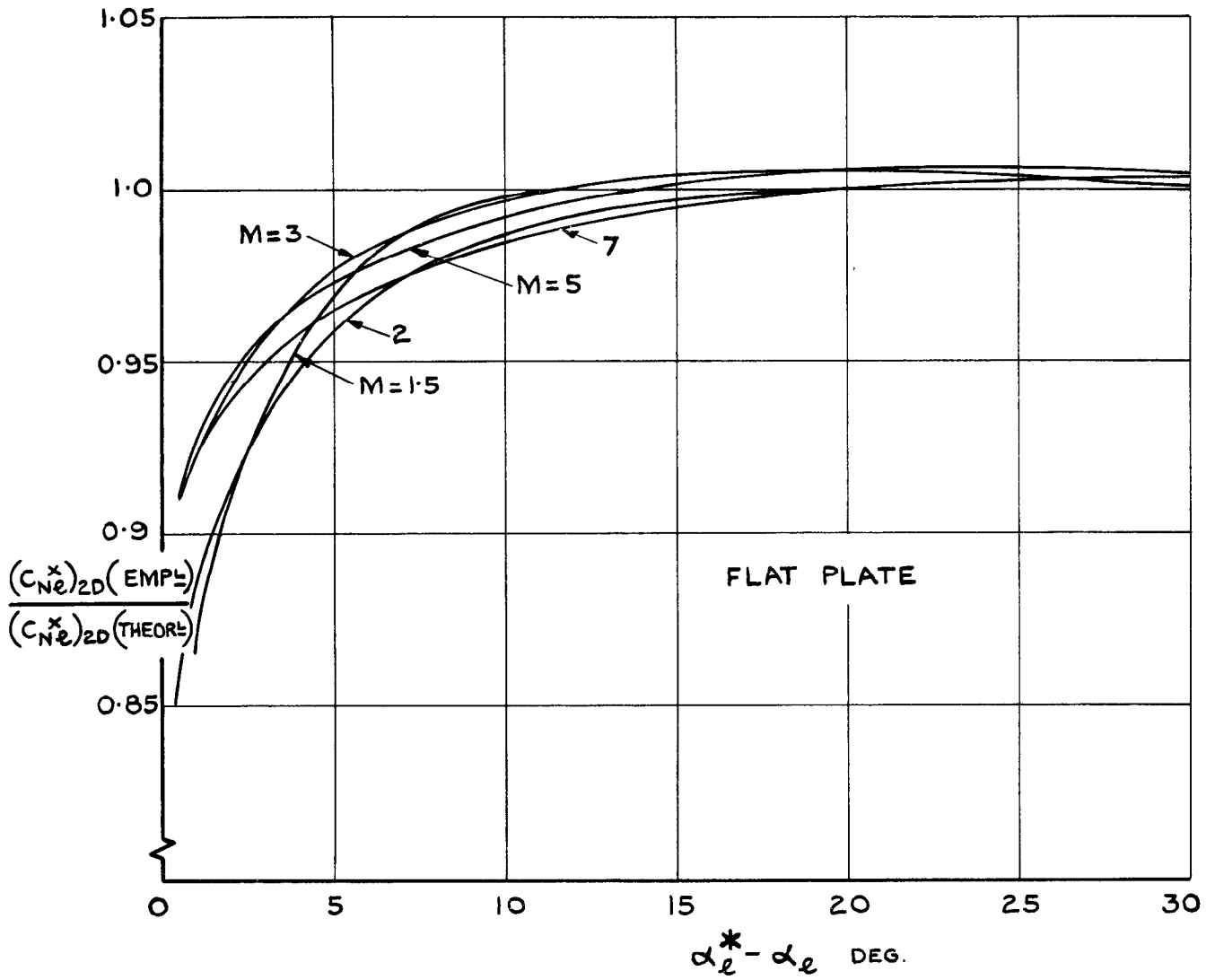


FIG.9. RATIO OF C_{Ne}^x IN TWO-DIMENSIONAL FLOW, AS ESTIMATED BY EQUATION (19) AND BY OBLIQUE SHOCK EQUATIONS.

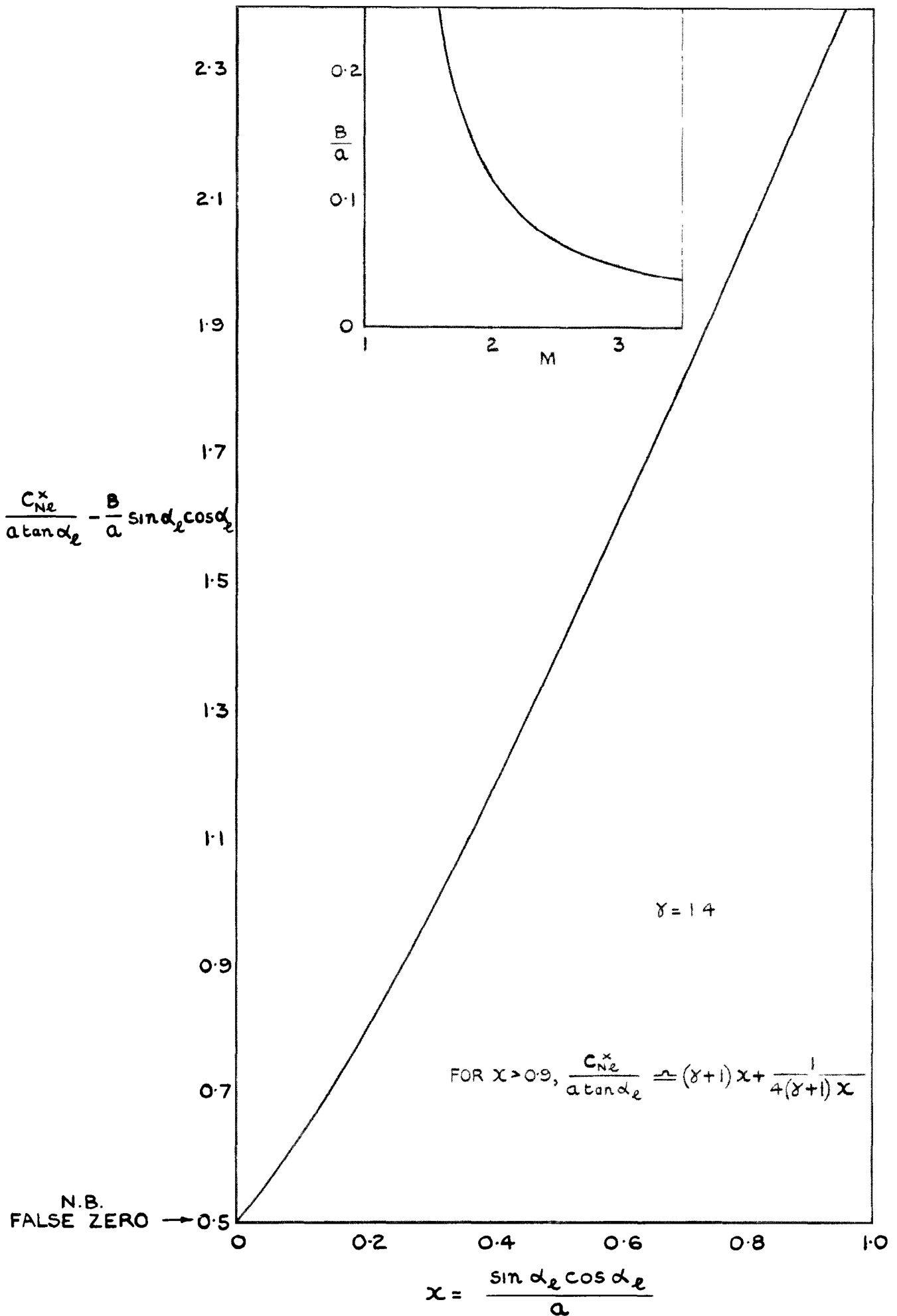


FIG. 10. NORMAL FORCE COEFFICIENT ON THE LOWER SURFACE OF THIN, SHARP-EDGED WINGS WITH LE SHOCK ATTACHED.

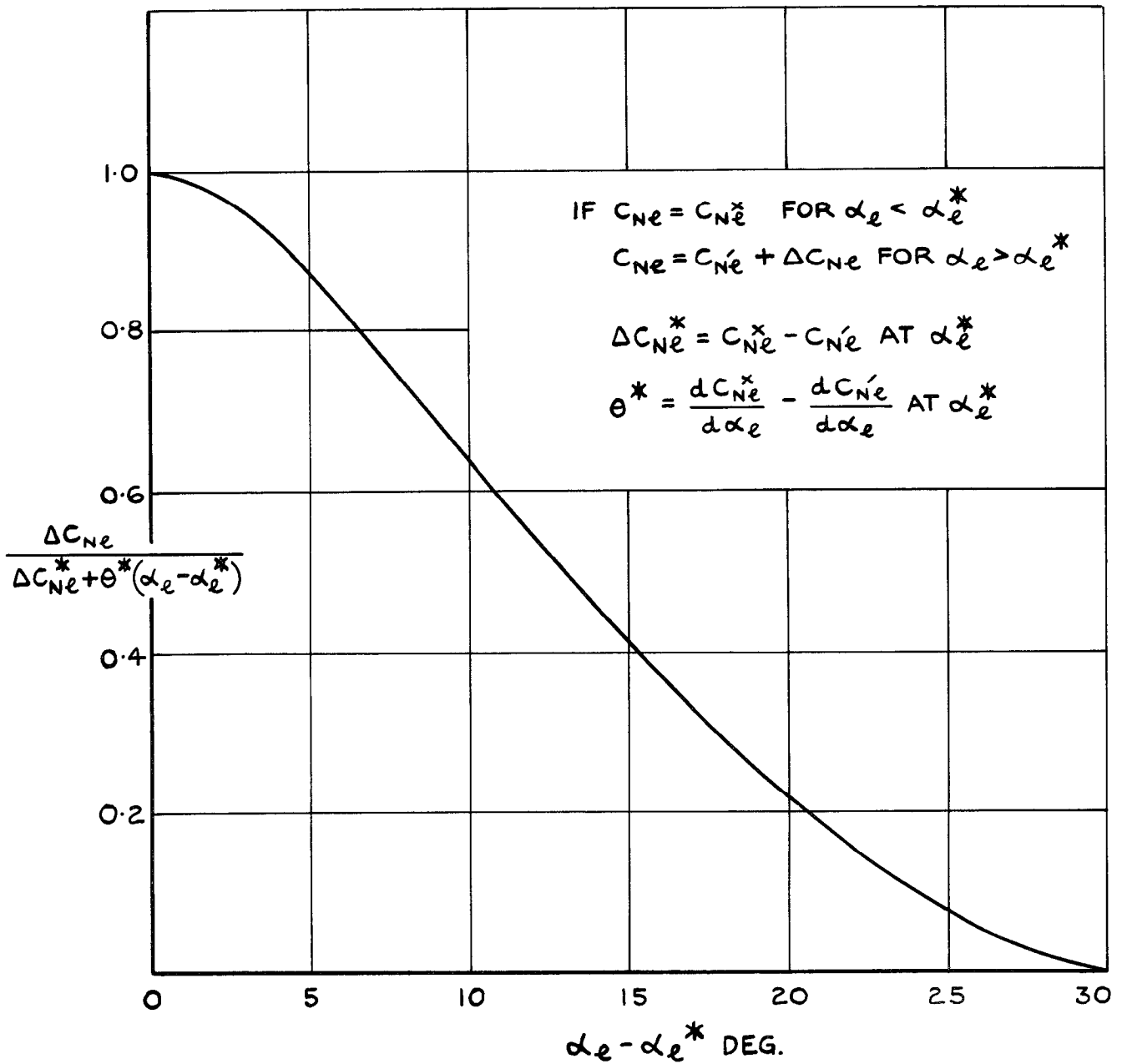


FIG.II. LOWER SURFACE NORMAL FORCE AT ANGLES ABOVE SHOCK DETACHMENT.

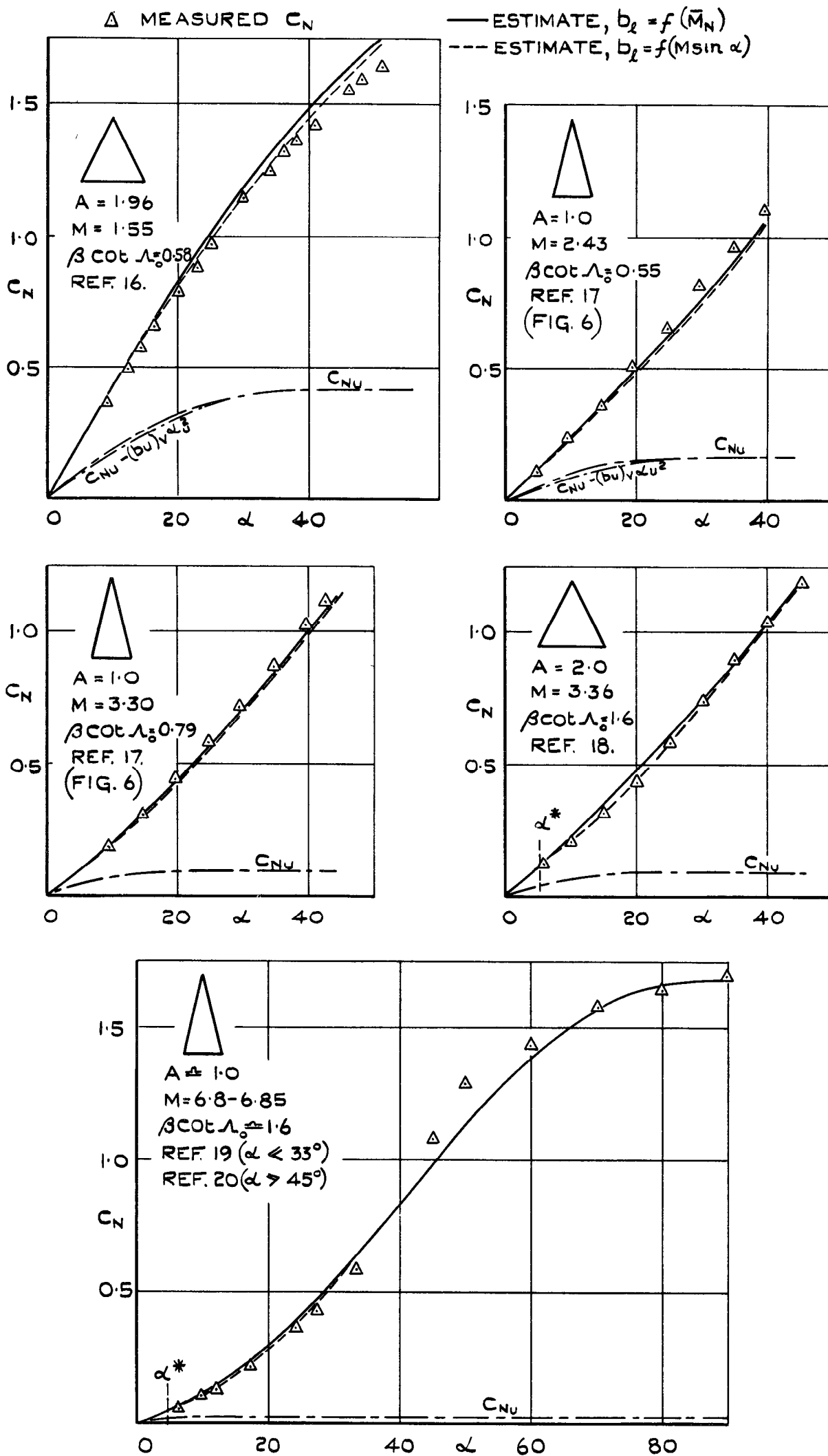


FIG. 12. COMPARISON BETWEEN ESTIMATED & MEASURED C_N vs. α FOR DELTA WINGS WITH L.E. SHOCK DETACHED, OR α_l^* SMALL.

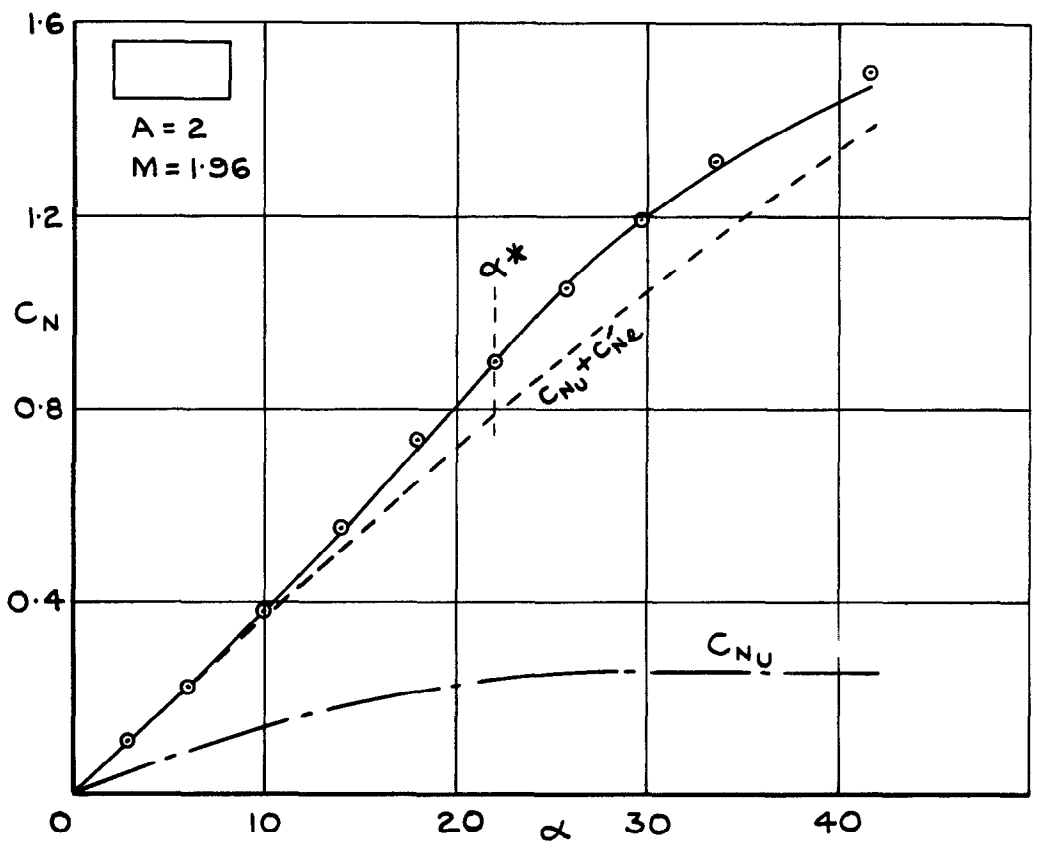
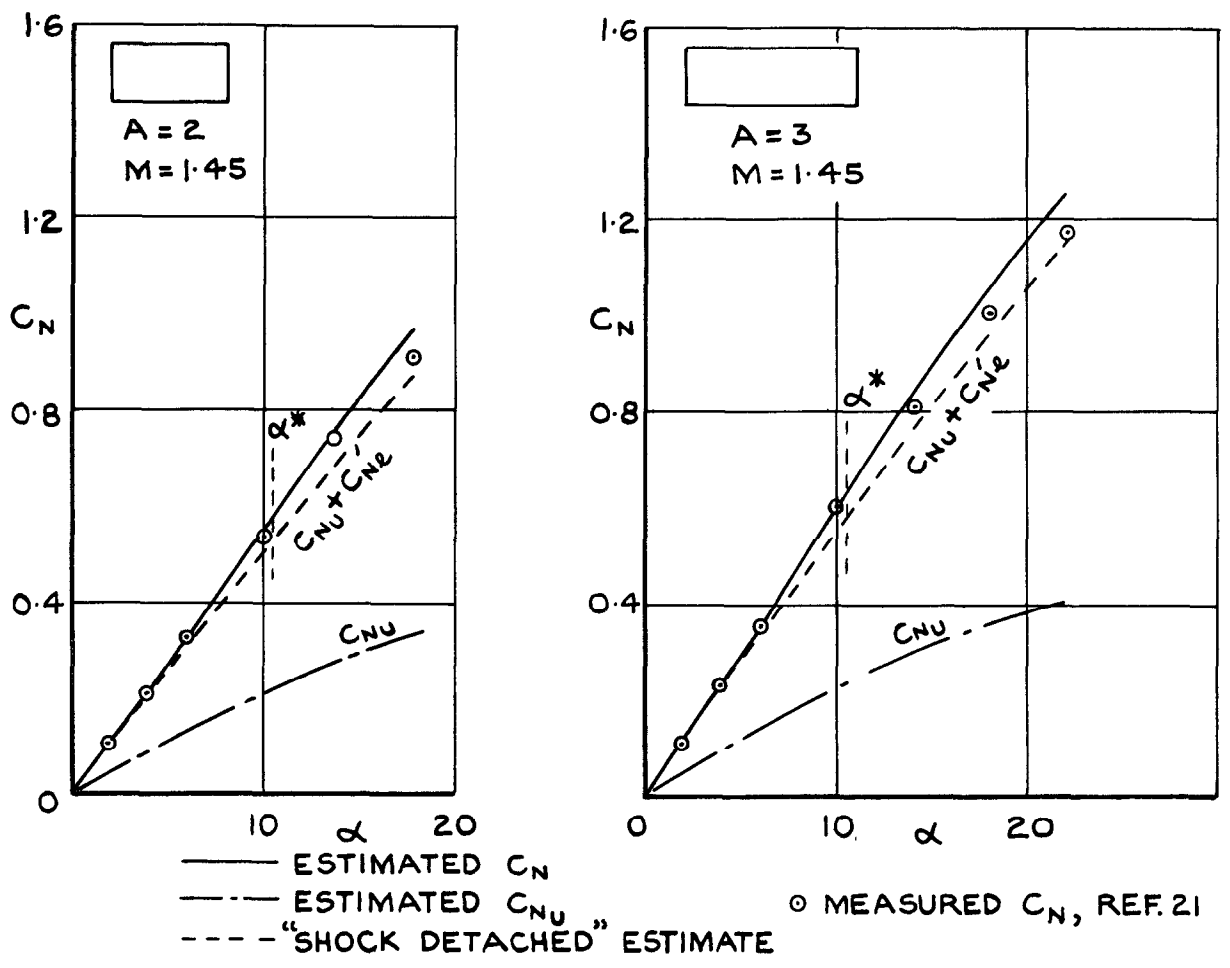
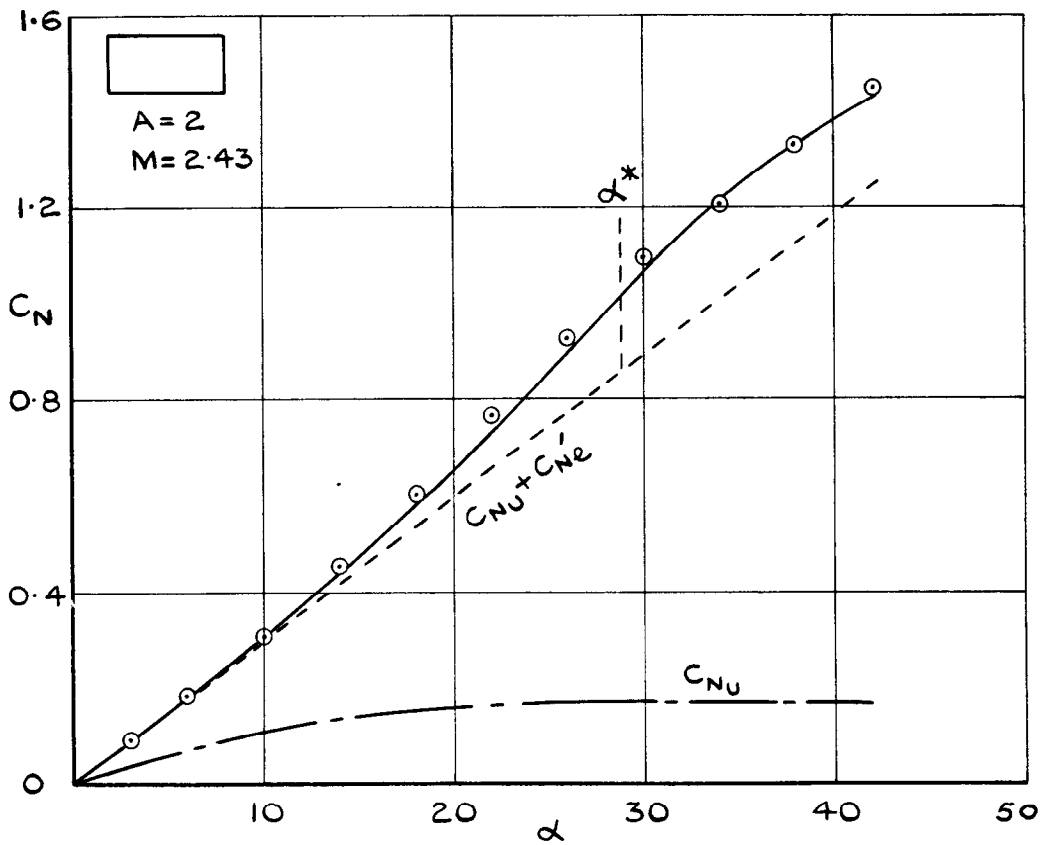


FIG.13. COMPARISON BETWEEN ESTIMATED AND MEASURED C_N vs α FOR WINGS WITH $\alpha_e^* > 5^\circ$ (L.E. SHOCK ATTACHED CASE).
(a) RECTANGULAR WINGS, $\beta A > 2$



— ESTIMATED C_N
 - - - ESTIMATED C_{N_U}
 - - - "SHOCK DETACHED" ESTIMATE

○ MEASURED C_N REF. 21

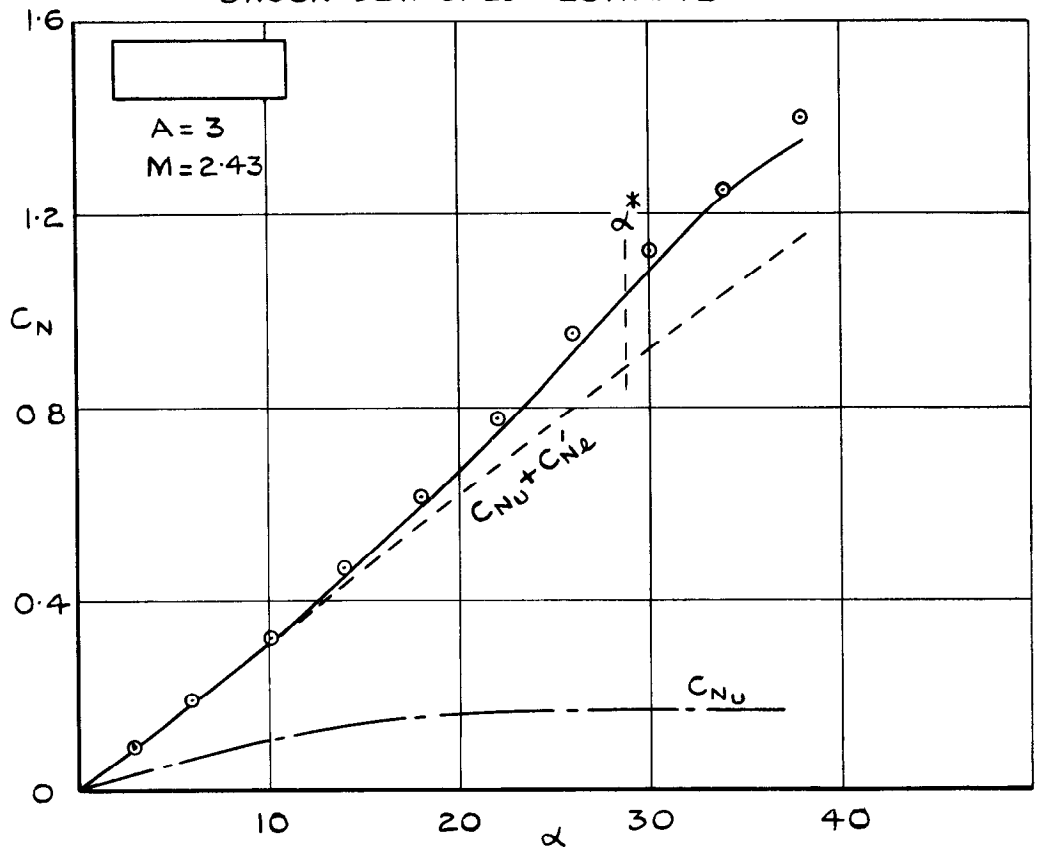


FIG.13 (cont'd). COMPARISON BETWEEN ESTIMATED AND MEASURED C_N vs α FOR WINGS WITH $\alpha_e^* > 5^\circ$ (L.E. SHOCK ATTACHED CASE).

(a) RECTANGULAR WINGS, $\beta A > 2$

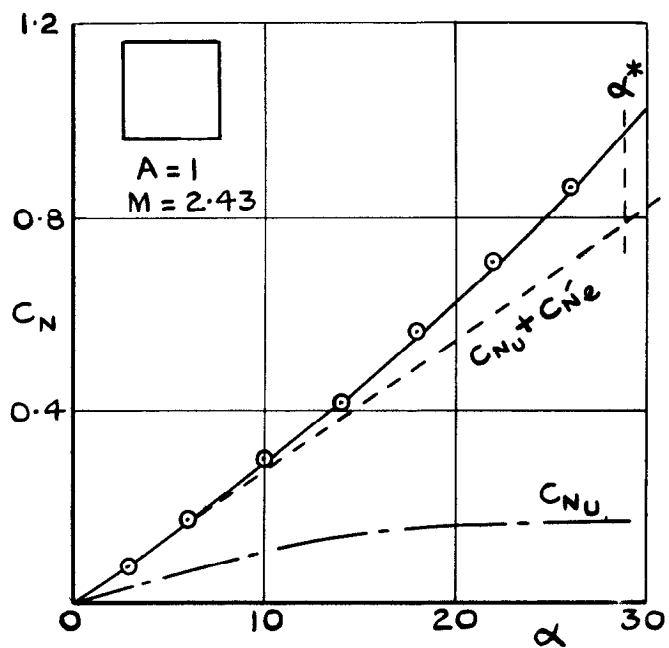
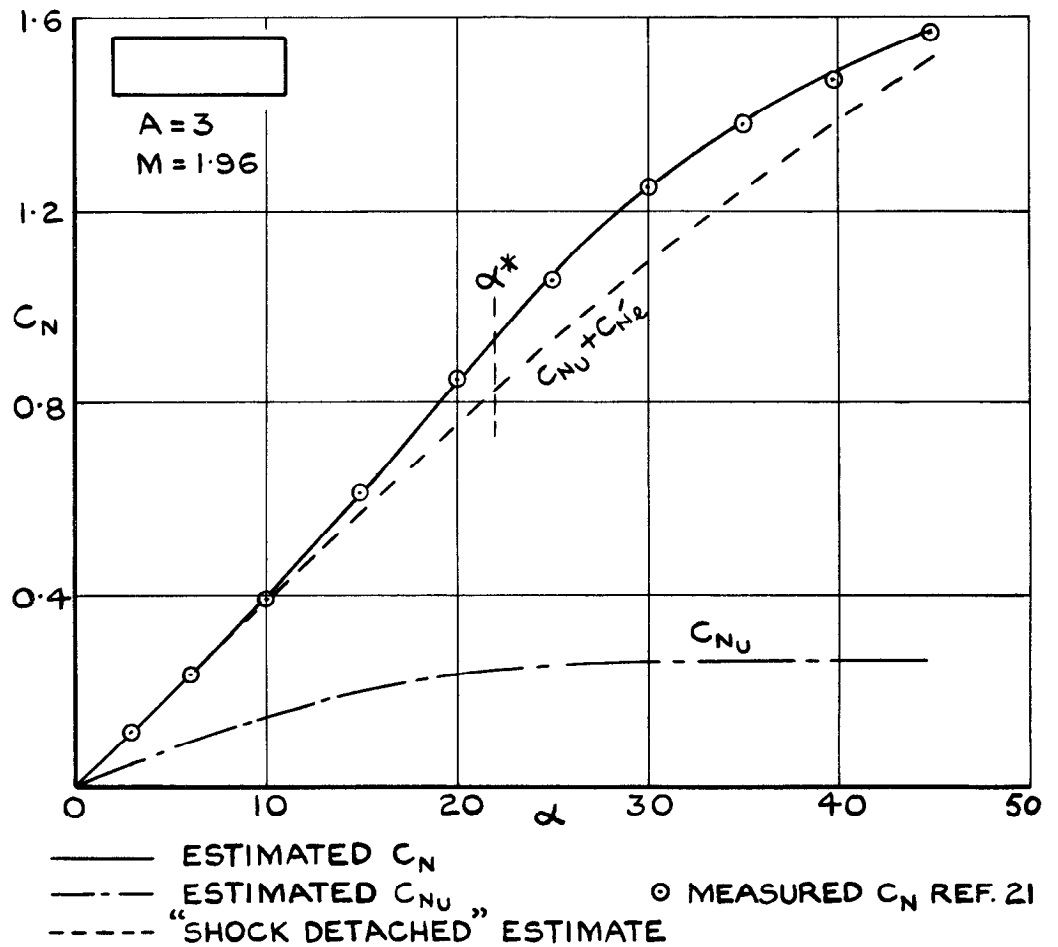


FIG.13 (cont'd). COMPARISON BETWEEN ESTIMATED AND MEASURED C_N vs α FOR WINGS WITH $\alpha_l^* > 5^\circ$ (L.E. SHOCK ATTACHED CASE)
(d) RECTANGULAR WINGS, $\beta A > 2$

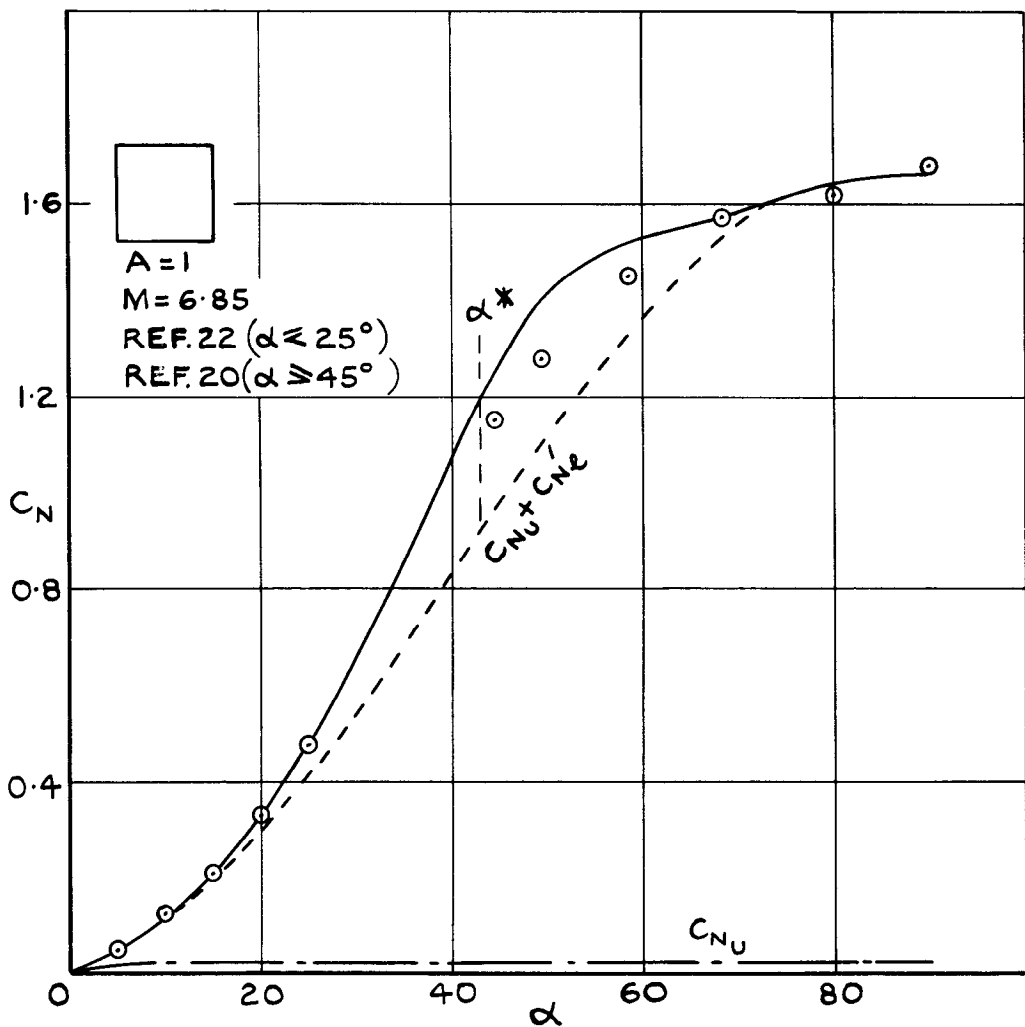
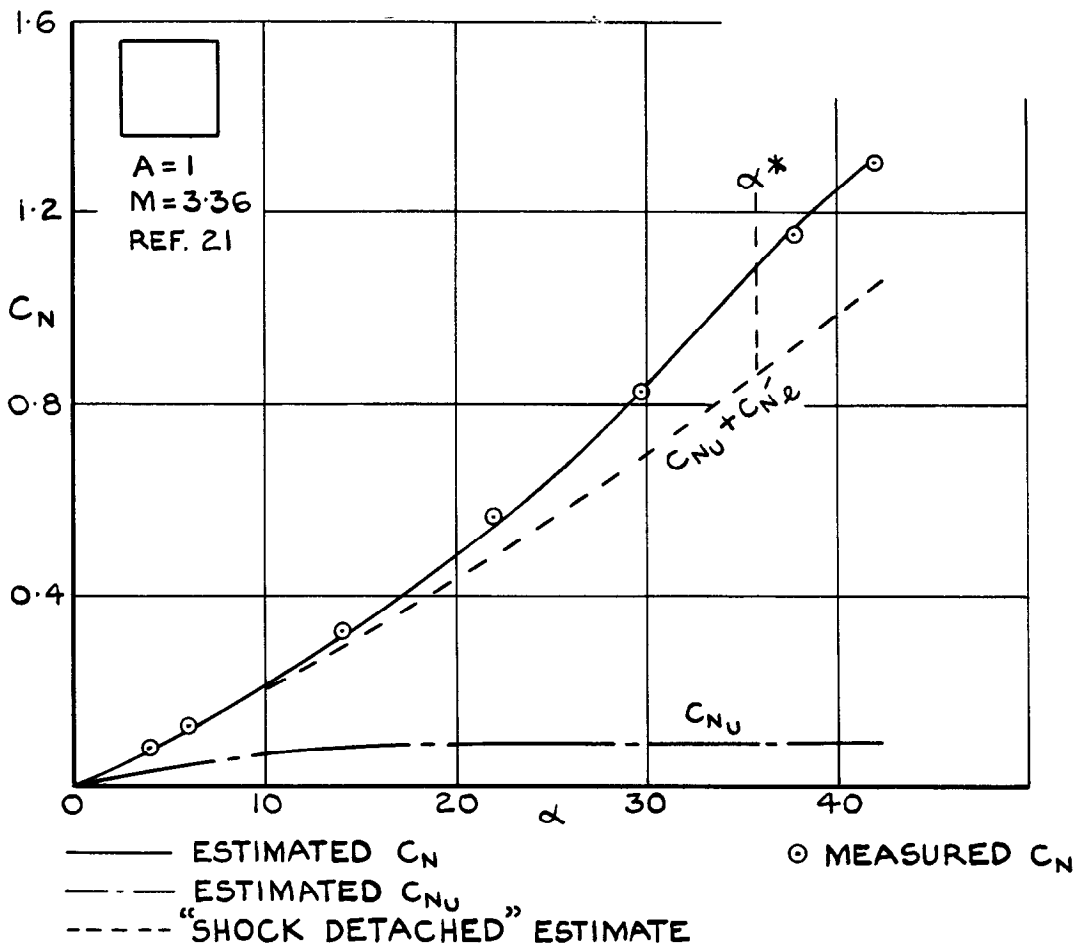
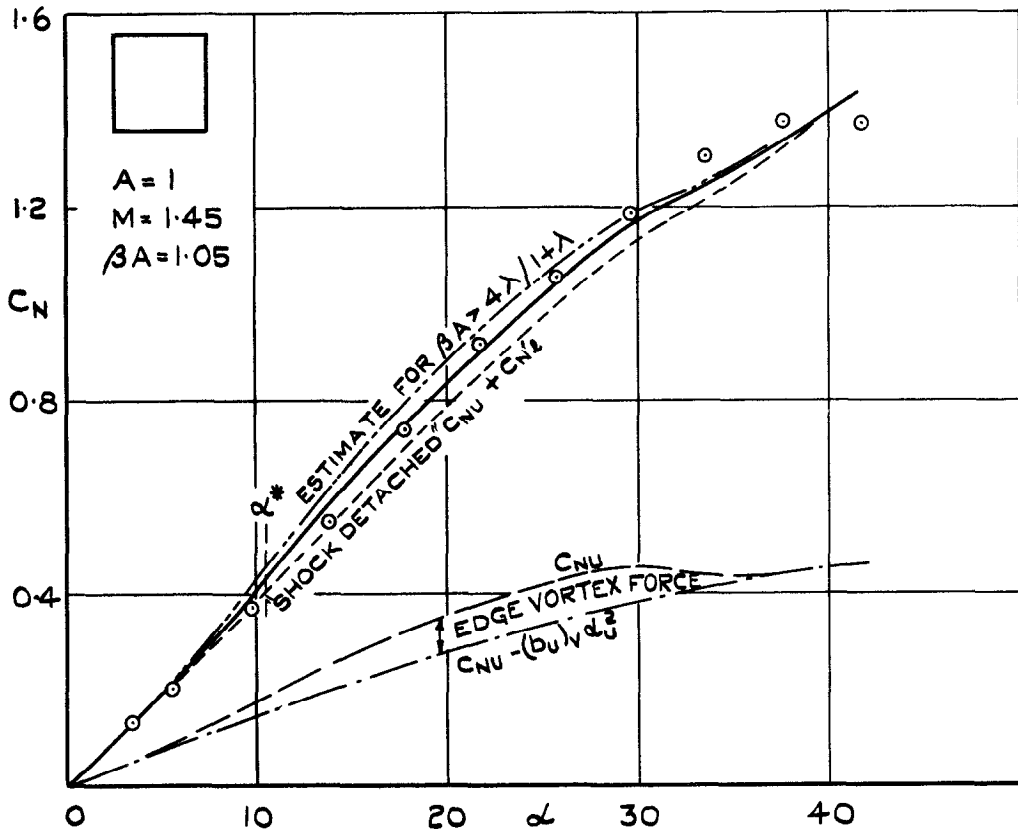


FIG.13 (cont'd). COMPARISON BETWEEN ESTIMATED AND MEASURED C_N vs α FOR WINGS WITH $\alpha_e^* > 5^\circ$ (L.E. SHOCK ATTACHED CASE)
(a) RECTANGULAR WINGS, $\beta A > 2$



— ESTIMATED C_N . \circ MEASURED C_N REF. 21.

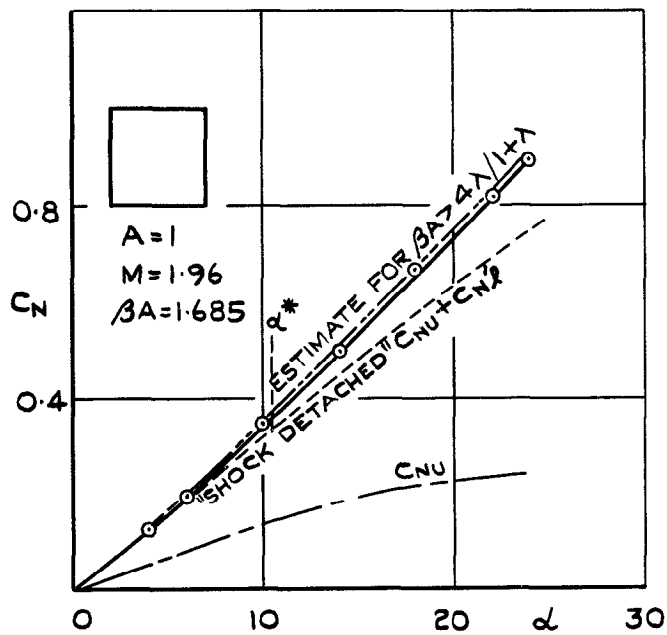


FIG.13.(cont,d) COMPARISON BETWEEN ESTIMATED AND MEASURED C_N vs α FOR WINGS WITH $\alpha_{\ell}^* > 5^\circ$ (L.E. SHOCK ATTACHED CASE.)
 (b) RECTANGULAR WINGS, $\beta A < 2$ (INTERFERING TIPS)

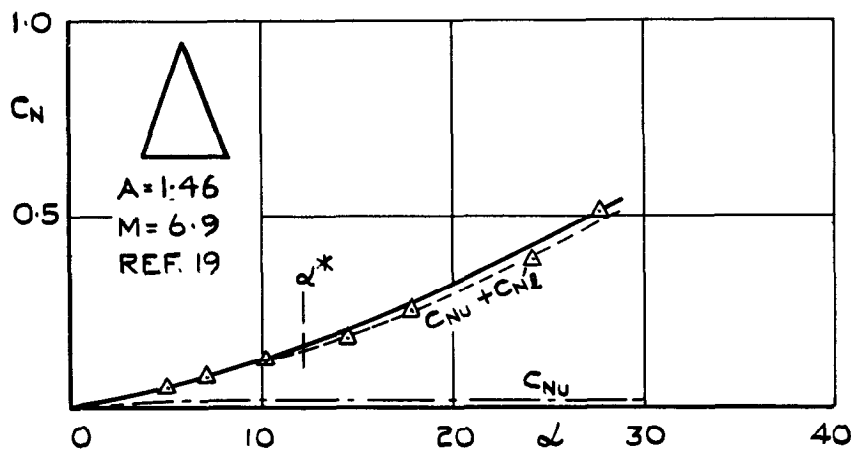
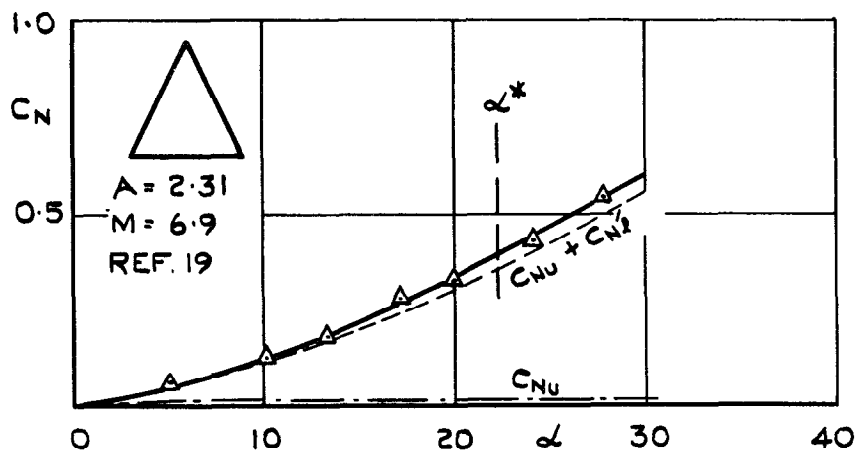
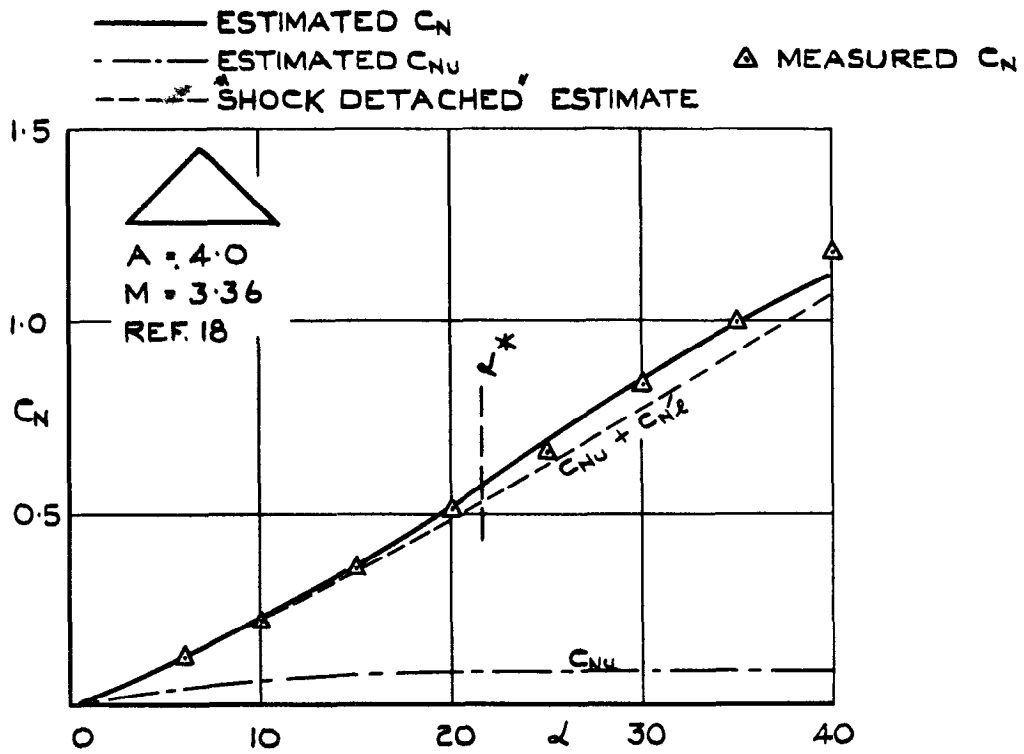


FIG.13.(cont'd) COMPARISON BETWEEN ESTIMATED AND MEASURED C_N vs α FOR WINGS WITH $\alpha_{l^*}^* > 5^\circ$
 (L.E. SHOCK ATTACHED CASE.)
 (C) DELTA WINGS.

A.R.C. C.P. No.662

533.693 :
533.6.011.5 :
533.6.013.13

AN EMPIRICAL PREDICTION METHOD FOR NON-LINEAR NORMAL FORCE
ON THIN WINGS AT SUPERSONIC SPEEDS. Collingbourne J.R. January, 1962

Theoretical and experimental results are used to produce a coherent 'engineering' method for predicting normal force on thin sharp-edged wings at supersonic speeds, the initial force curve slope being known. The method can be applied at angles up to 90° and, in principle, to any planform, although most of the results used to develop the method are for delta and rectangular wings.

A summary of the method is given in section 5.

A.R.C. C.P. No.662

533.693 :
533.6.011.5 :
533.6.013.13

AN EMPIRICAL PREDICTION METHOD FOR NON-LINEAR NORMAL FORCE
ON THIN WINGS AT SUPERSONIC SPEEDS. Collingbourne J.R. January, 1962

Theoretical and experimental results are used to produce a coherent 'engineering' method for predicting normal force on thin sharp-edged wings at supersonic speeds, the initial force curve slope being known. The method can be applied at angles up to 90° and, in principle, to any planform, although most of the results used to develop the method are for delta and rectangular wings.

A summary of the method is given in section 5.

A.R.C. C.P. No.662

533.693 :
533.6.011.5 :
533.6.013.13

AN EMPIRICAL PREDICTION METHOD FOR NON-LINEAR NORMAL FORCE
ON THIN WINGS AT SUPERSONIC SPEEDS. Collingbourne J.R. January, 1962

Theoretical and experimental results are used to produce a coherent 'engineering' method for predicting normal force on thin sharp-edged wings at supersonic speeds, the initial force curve slope being known. The method can be applied at angles up to 90° and, in principle, to any planform, although most of the results used to develop the method are for delta and rectangular wings.

A summary of the method is given in section 5.

© *Crown Copyright 1963*

Published by
HER MAJESTY'S STATIONERY OFFICE

To be purchased from
York House, Kingsway, London w.c.2
423 Oxford Street, London w.1
13A Castle Street, Edinburgh 2
109 St. Mary Street, Cardiff
39 King Street, Manchester 2
50 Fairfax Street, Bristol 1
35 Smallbrook, Ringway, Birmingham 5
80 Chichester Street, Belfast 1
or through any bookseller

S.O. CODE No. 23-9013-62

C.P. No. 662